Final Report

Review of AI Avian Monitoring with CCTV Cameras on Floating Wind Turbines

May 2025

Summary

Location: Hywind Tampen Floating Windfarm Norway

Number of cameras: Three

Survey Duration: May 2023 to November 2024

Hours of video analysed: 8,252

Total bird observations: 2,197

Bird classification:

- 1,948 (89 %) classified to order
- 1,922 (87 %) classified to family level
- 1004 (46 %) classified to species level

Norwegian Red List *Endangered* birds identified: Black-legged kittiwake

Norwegian Red List *Vulnerable* birds identified: European Herring Gull

Three CCTV cameras were installed within the Hywind Tampen Floating Offshore Wind Farm in Norway for the purpose of Health, Safety and Environmental Monitoring. However, the data collected by these cameras also offer the potential to collect data on the presence, abundance and behaviour of birds within the offshore wind farm. To investigate this, Equinor partnered with Spoor to rapidly scale this approach, and contribute to filling key gaps in our understanding of bird movements in and around offshore wind farms.

Data were collected over 19 months from May 2023 – November 2024, and in total 2,197 birds were detected over 8,252 hours of monitoring. Of these, 89% were classified to order level, 87% to family level and 46% to species level. The dataset was dominated by large gulls (*Larus* spp.), in particular the Great Black-backed Gull *Larus marinus.*

In collaboration with The Biodiversity Consultancy, the resultant data were analysed to investigate patterns in abundance, flight heights and flight directions. Annual patterns in abundance, with the number of birds recorded peaking during summer months, became apparent after data were normalized to account for recording duration and camera field of views were standardized to cover an equal detection space. Weather conditions did not appear to strongly influence observations, though this is likely to reflect the distance to the weather station from which data were available.

Analyses of flight height data indicated that the majority of recorded birds were at collision risk height. However, this is likely to reflect the fact that minimum height covered by the camera field of view was approximately 19 m above sea-level, consequently lower flying birds would not be detected. As might be expected given the propensity for many of the species detected in this study to fly close to the sea surface, mean flight heights were typically close to the lower limit of the field of view of the cameras.

Seasonal and spatial differences were detected in species recorded flight directions. More directional flight was detected by the camera collecting data outside the wind farm than was the case for the two cameras within the wind farm. Similarly, there was evidence of more directional flight, along a North-West to South East axis, during the periods associated with spring migration, likely to reflect birds returning to their breeding grounds.

To better understand the applicability of the approach, data were further investigated in order to determine the extent to which assumptions made in processing may influence the uncertainty, bias, error and precision of the resulting observations. A key focus for these analyses was the impact of an assumption of a standard 1 m wingspan across all species on estimates of species flight heights and the distance between the bird and camera. This assumption introduced a systematic error and bias into both estimates. As the most abundant species recorded have wingspans in excess of 1 m, both values were underestimated. However, as our analyses highlighted, these errors could be reduced through the use of species specific estimates of wingspan.

The results presented in this report highlight the potential value of data collected using CCTV cameras for contributing to a greater understanding of bird interactions with offshore wind farms. Whilst challenges remain in the interpretation of the resulting data, these can be addressed by using cameras with a standardized field of view within each study, and by basing estimates of distance and flight height on species-specific wingspan estimates where possible.

Table of contents

Introduction and background

Equinor and Spoor have partnered to deploy Spoor AI bird-monitoring technology on Hywind Tampen, filling a data gap on bird activity offshore. The collection and analysis of these data is expected to inform biodiversity risk and ensure that offshore wind is planned and operated in environmentally responsible ways.

Uniquely, this project uses AI to process videos from CCTV cameras which were pre-installed on the floating wind turbine service platforms (initially intended to monitor Health, Safety, and Environment activities). This innovative configuration means that greater value can be captured from the same hardware performing two different functions. Although the CCTV cameras are lower resolution (and therefore range) than the cameras which Spoor typically use, this project has the potential to enable the collection of bird-activity and species identification (ID) data from offshore assets which have CCTV cameras installed. This would enable a rapid scaling of bird activity data-gathering offshore which has the potential to make a huge contribution to the state of the science and of the offshore wind industry worldwide. This report is a follow-up to the original pilot study[1] with an aim of better understanding sources of variability, bias, error and uncertainty in the data collected.

Hywind Tampen

Hywind Tampen is the largest floating wind farm in the world, located 140 km off the Norwegian coast, (see Figure 1) with a capacity of 88 MW, provided by eleven 8.6 MW Siemens Gamesa wind turbines. The project directly reduces emissions from oil and gas production on the Snorre and Gullfaks offshore fields by approximately 200,000 tonnes of CO_2 and 1,000 tonnes of NO_x emissions per year.

Hywind Tampen is Norway's first full scale offshore wind farm and has a critically important role to play in the development of the Norwegian offshore wind industry and the global expansion of floating offshore wind, which Equinor pioneered. From a biodiversity perspective, Hywind Tampen provides a unique opportunity to gather bird activity data off the coast of Norway and start building a knowledge base to understand and protect vulnerable species as they interact with industrial windfarm development.

[1] Pilot Report Spoor - AI Avian Monitoring with CCTV Cameras on Floating Wind Turbines Experiences and Future Potential Available online at: https://cdn.equinor.com/files/h61q9gi9/global/26cc50b23fe8e28e10f9cc74c2dad1d20dae188a.pdf?pilot-report-avian-monitoring-on-floating-wind-turbines-2024-equinor.pdf

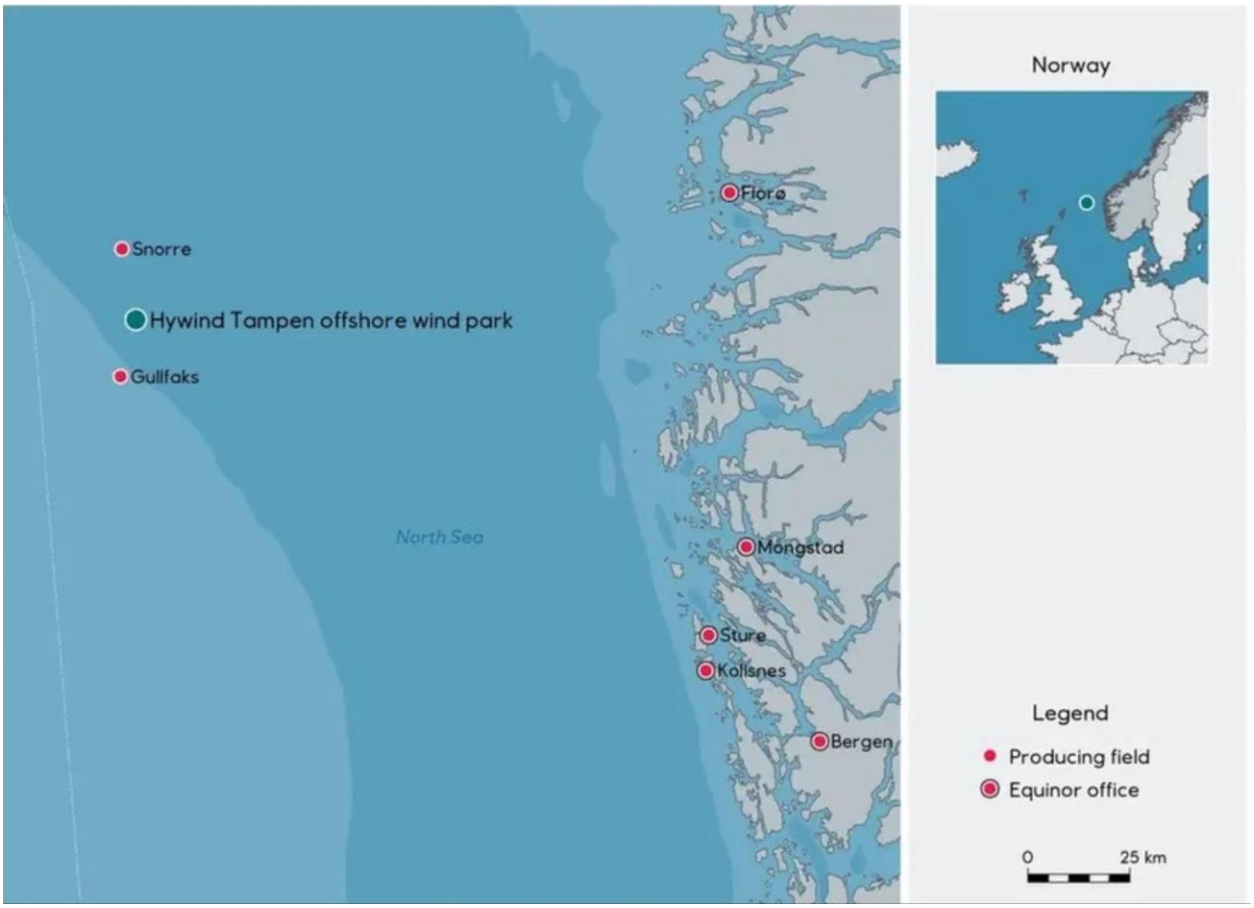

Figure 1: Courtesy of Equinor: Hywind Tampen (n.d)*, showing the location of the Hywind Tampen wind farm, 140 km off the Norwegian west coast.*

About Spoor

Spoor is a Norwegian biodiversity technology company, with a vision to enable nature and industry to coexist. Spoor promotes biodiversity positive wind energy development by combining high-resolution video cameras with advanced AI-based software to detect, track and identify birds and analyse their activity. This kind of accurate, detailed empirical data can reduce environmental and financial risks and allow smarter decision making by developers and regulators. Spoor currently employs 22 people of diverse backgrounds; with 14 nationalities and a 36% female representation. The team's expertise includes ornithology, offshore wind, regulatory affairs, data science, edge computing, and machine learning. Since the first pilot was launched in March 2021, Spoor's solution has been deployed on multiple onshore and offshore sites in Northern Europe, with further installations underway. Together with Equinor and Fugro in a separate project, Spoor pioneered the use of floating offshore platforms offshore to monitor bird-activity for pre-construction surveys.

About The Biodiversity Consultancy

The Biodiversity Consultancy is a specialist consultancy in biodiversity risk management. We work with sector-leading clients to integrate nature into business decision-making and design practical environmental solutions that deliver nature-positive outcomes. We provide technical and policy expertise to manage biodiversity impacts at a project level and enable purpose-driven companies to create on-the-ground opportunities to regenerate our natural environment. As strategic advisor to some of the world's largest companies, we lead the development of post-2020 corporate strategies, biodiversity metrics, science-based targets, and sustainable supply chains. Our expertise is applied across the renewable energy sector, including hydropower, solar, wind, and geothermal, where we specialise in the interpretation and application of international finance safeguards.

Aims and objectives

This report will set out the key results and birds observations collected over 19 months (May 2023 – November 2024) of monitoring at Hywind Tampen Offshore Wind Farm. This will include a description of the species observed and discussion of the seasonal patterns in abundance and flight direction. To facilitate comparison between data collected using cameras with different sampling volumes, we develop approaches to produce normalised estimates of abundance from the available data. Using these estimates, we will analyse the data in relation to temporal and environmental variables in order to quantify the uncertainty introduced into the data as a consequence of these. Finally, we will consider how assumptions made in relation to the body size of birds may impact the precision of the available data, with particular reference to factors that may influence assessments of species collision risk.

Methods

Data capture

Surveillance cameras as sensors

Spoor AI utilises cameras as sensors for data capture. Spoor AI software is hardware agnostic and can process video from any commercially available high-resolution camera. This allows for flexible, lightweight and cost-effective infrastructure. The AI software is adapted to analyse data from both stable and unstable (floating turbines/buoys) vantage points.

Camera-based monitoring is a non-intrusive technology that will not interfere with any other installations. It is also a non-intrusive *methodology* that has minimal interference with the environment and species it is monitoring, and therefore introduces a minimum of sampling biases compared to human observers.

To date, Spoor has worked with surveillance video cameras from AXIS, Avigilon and Eaton (Hernis) with both wide-angle dome cameras and classic bullet cameras. Surveillance cameras are affordable and are designed to record continuously for years at a time. They have custom built water and weatherproof housings that are durable in tough weather conditions. One current disadvantage is that they are designed for security rather than scientific purposes, so that certain settings (like focus and focal length, frame rate per second, multi-camera time syncs) are simplified and need to be adjusted by Spoor's engineers. However, both these settings and the general quality and performance of the cameras are being improved by the camera manufacturers on a continuous basis.

The choice of camera, lens, housing and other equipment is decided on a case-by-case basis. Various aspects like cost, durability in different environments, focal distance, and field of view need to be considered in relation to the project specific purpose of monitoring.

A number of variables within the equipment determine the ability and quality of bird detection, some examples being sensor resolution, focal length, lens "speed" (f-stop), shutter speed, frame rate (Frames Per Second, FPS), and data bitrates.

Using cameras for data capture yields both advantages and limitations. Some of the limitations are:

- Visible Imaging Sensor cameras cannot detect without daylight. For 24 hour monitoring they can be combined with thermal imaging cameras.
- Image quality is affected by weather; fog, rain and snow will typically reduce the range. Direct sun striking an unclean lens can also degrade the image quality. In addition, atmospheric quality like humidity, airborne dust or air pollution affects image quality especially onshore.

- Range is ultimately restricted by the physics of lenses and the stability of the mounting location. The longer the focal length, the more likely it is that any vibration will degrade the final video image (e.g. from wind against the camera body, or the vibration of a working wind turbine).

In addition to cameras, a power supply is needed for them in order to function, and a network connection is needed for data transmission. In certain cases where internet access is not available, data needs to be stored onsite and manually retrieved at a later date.

The Hernis CCTV cameras

This pilot study used three outdoor CCTV cameras mounted on three floating wind turbines. The cameras had originally been selected for the purpose of HSE monitoring of personnel doing operational and maintenance work on the turbines.

Figure M1: The Hernis CCTV camera, illustration retrieved from Hernis (n.d.)

The CCTV cameras were manufactured by Hernis (see Figure M1). They have resolution of 1920x1080 pixels, a 30x optical zoom lens (4.5-135 mm focal lengths), and a frame rate of 30 frames per second. The view angle is between 2.35° and 65.1°. The cameras have wipers to clean the lens for water and other contamination. The settings and camera orientations can be remotely controlled and adjusted.

Vantage points and camera settings

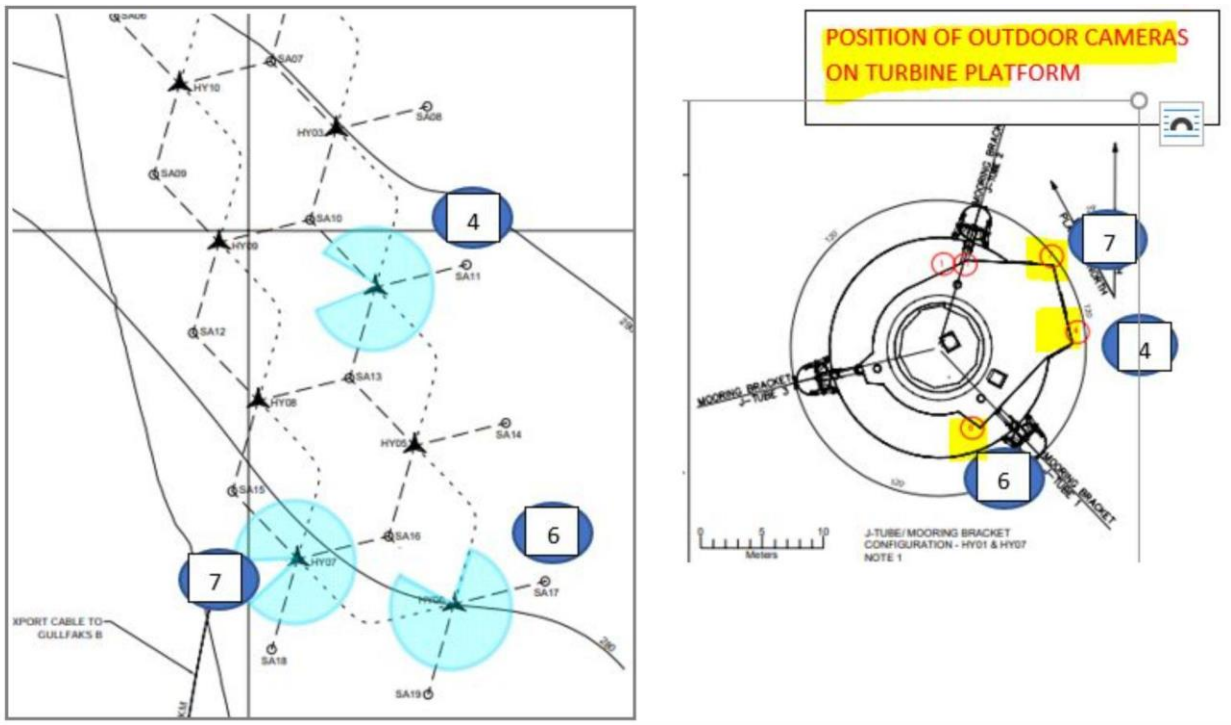

Figure M2: The vantage points of the outdoor CCTV cameras for each of the three turbines in question. The light blue circles indicate the potential field of view. For certain angles, the turbine tower obstructs the view.

The CCTV cameras at Hywind Tampen have been installed for the purpose of HSE monitoring of human operations at the turbine, and the vantage points were selected to optimise for this, and not for bird monitoring – but remote control made it possible to use the cameras for both purposes. In addition, camera placement needs to adhere to safety regulations and should not interfere with turbine operations. The placement of the cameras on the three turbines are shown in Figure M2.

The exact position of each camera is measured by the yaw, pitch and roll angles, as seen in Figure M3.

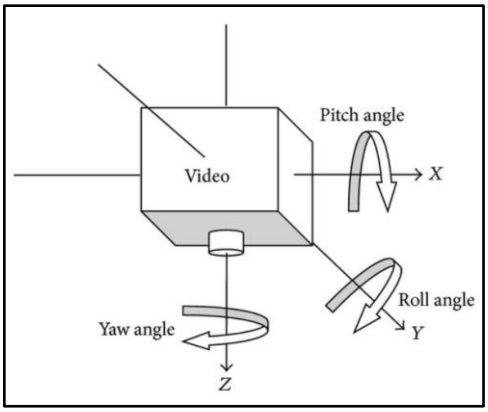

Figure M3: The yaw, pitch and roll angles that describe the position of a camera. Illustration from Zhang *et al*. (2014).

Spoor estimated the yaws, pitches and rolls of each camera based on landmarks visible in the images. These estimates were confirmed as reasonable by Equinor.

The cameras are mounted outside the railing on the turbine platform, as seen in Figure M4. This allows for orienting the camera towards the sea to optimise for bird monitoring, when they are not used for HSE monitoring. Figure M5 shows examples of the camera positions used for HSE monitoring and for bird monitoring, respectively.

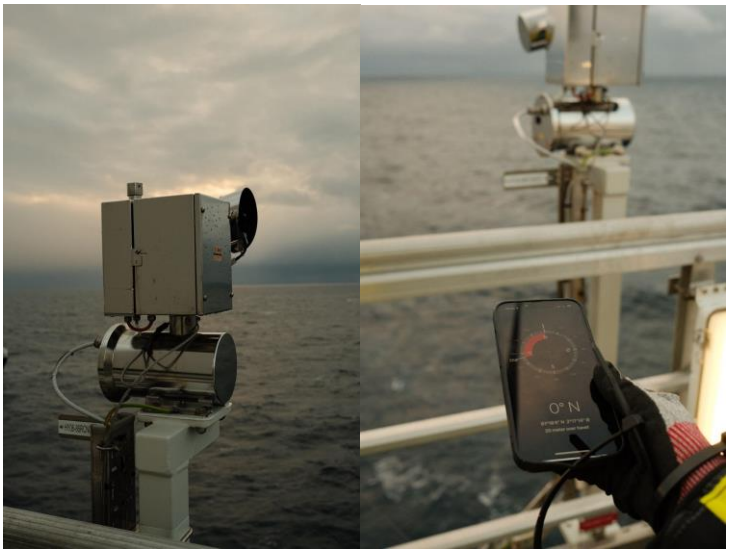

Figure M4: The CCTV camera mounted on turbine HY06. Pictures taken by an Equinor operations engineer 7 March 2024.

Figure M5: Two positions of the camera at turbine HY06: The HSE-position (left) and the bird monitoring position (right).

The cameras were programmed by Equinor's staff so that each camera returns to the bird monitoring position whenever it is not being used for HSE purposes. Figure M6 illustrates the fixed bird monitoring position of each camera.

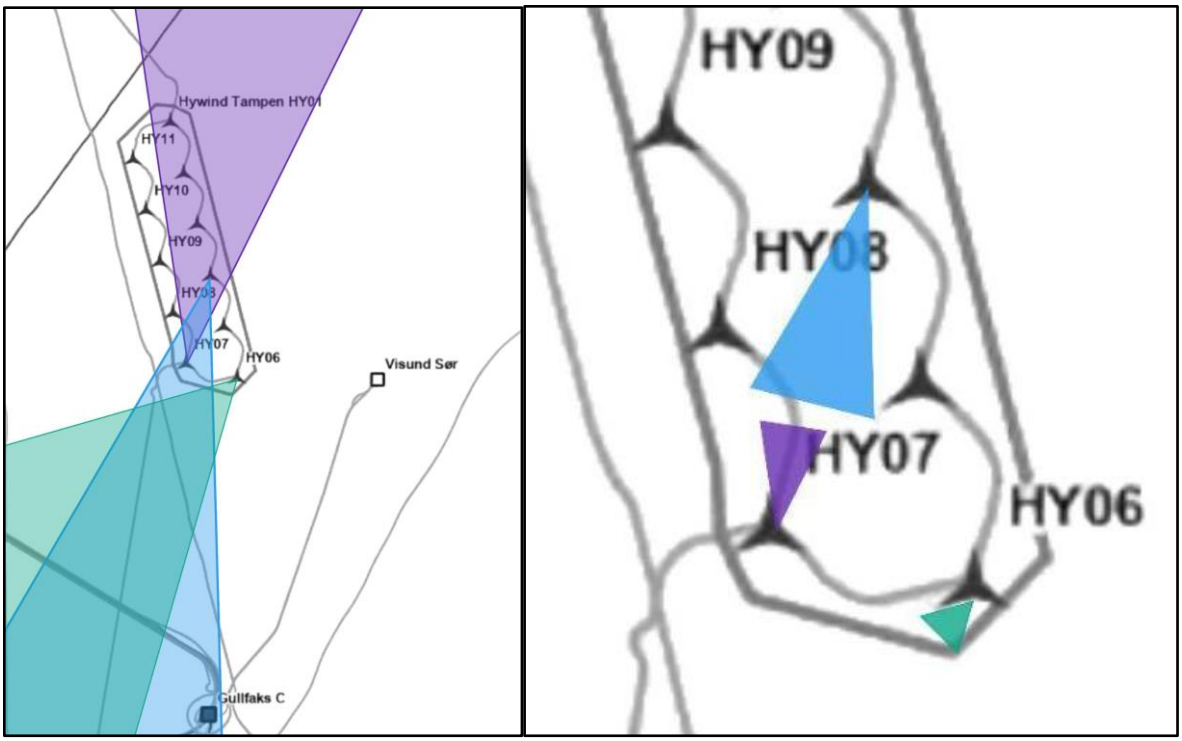

Figure M6: A representation of the camera orientations for the bird monitoring positions (left). The illustration is north/south oriented, with the Gullfaks oil field towards south. The detection range per viewpoint of a bird of 1 m wingspan is indicated by the coloured areas in the rightmost illustration.

The three vantage points selected for this pilot were on turbines HY04, HY06 and HY07, and the cameras were identified with numbers 8, 13, and 16 respectively. For the rest of this report, these will be referred to from north to south as viewpoint A (turbine HY04, camera 8), viewpoint B (turbine HY07, camera 16) and viewpoint C (turbine HY06, camera 13).

Viewpoint A

Facing south/south-west, from the vantage point of turbine HY04, the field of view is towards the middle of the wind farm, as seen in Figure M8. Turbine HY07 – viewpoint B – is in the middle of the field of view as seen in Figure M9. The distance between HY04 and HY07 is approximately 2.6 kilometres.

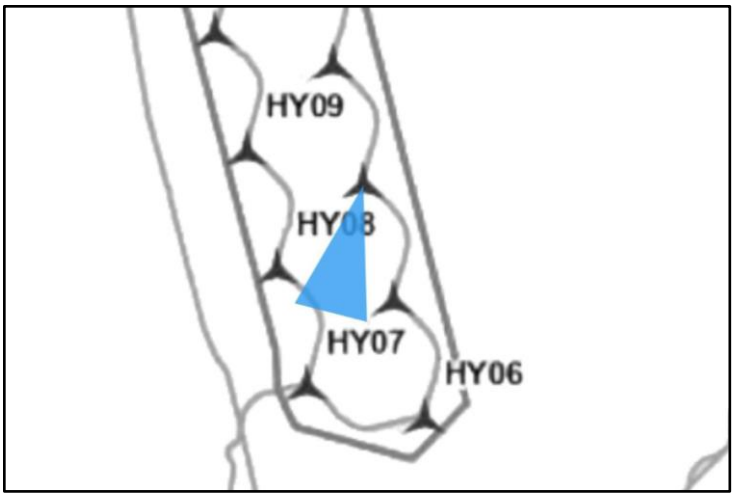

Figure M8: The camera orientation and position of viewpoint A, indicated in blue. The blue area illustrates the detection range of a bird with a 1 m wingspan.

Figure M9: The track of a Great Black-backed Gull captured from viewpoint A. Turbine HY07 (viewpoint B) is visible in the middle of the field of view. An oil platform in the Gullfaks field is visible behind HY07, a second is visible towards the leftmost side of the horizon.

Viewpoint B

As seen in Figure M10, the camera is facing north/north-east. From the vantage point of turbine HY07, the field of view is almost directly opposite viewpoint A and towards the middle of the wind farm (Figure M11).

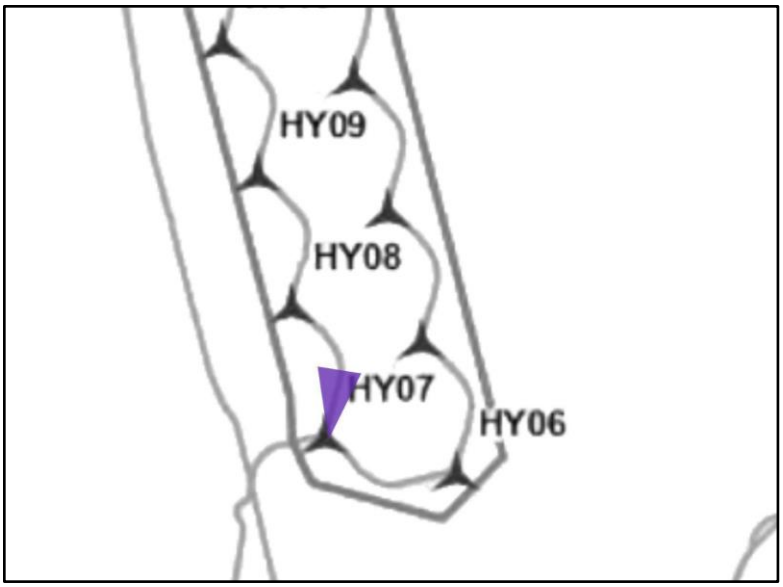

Figure M10: The camera orientation and position of viewpoint B, indicated in purple. The purple area illustrates the detection range of a bird of 1 m wingspan.

Figure M11: The track of a great black-backed gull (red dots) passing through the wind farm, as seen from viewpoint B. Turbines HY01 - HY04 are visible from left to right in the field of view.

Viewpoint C

As seen in Figure M12, the camera faces south-west, the same direction as viewpoint A. From the vantage point of turbine HY06, the field of view is the edge of the wind farm towards the open sea, as seen in Figure M13.

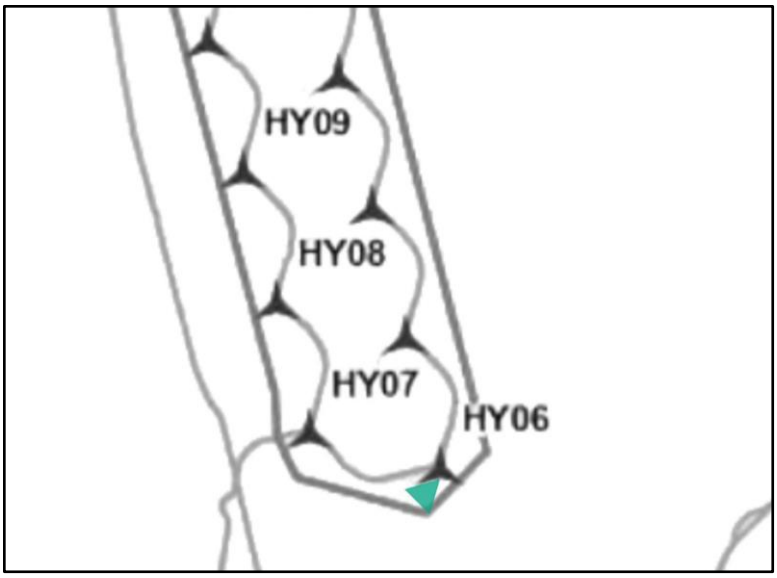

Figure M12: The camera orientation and position of viewpoint C, in green. The green area illustrates the detection range of a bird with a 1 m wingspan.

Figure M13: The track of a barn swallow captured from viewpoint C. Two oil platforms at the Gullfaks oil field are visible in the leftmost horizon.

Viewpoint properties

The cameras at each of the three viewpoints have different orientations and settings, as listed in Table M1. As discussed in the chapter *Surveillance cameras as sensors,* the camera properties, settings and orientation determine the maximum bird detection distance (range) and height

(altitude). On Hywind Tampen, the cameras have focal lengths ranging from 36 mm on viewpoint A to just 4.5 mm on viewpoint C. As stated in *The Hernis CCTV Cameras* chapter, the lowest possible focal length is 4.5 mm, while the highest is 135 mm. The difference in focal lengths translates directly to substantial differences in estimated maximum detection distance and height for each of the viewpoints. For a bird with a 1 m wingspan, the estimated detection distance for viewpoint A is ~1,500 m and for viewpoint C it is ~200 m.

Table M1: Parameters of the camera settings, ranges and orientations per viewpoint. The differences in focal lengths explains the notable differences in estimated detection distances for each viewpoint.

	Viewpoint A	Viewpoint B	Viewpoint C
Turbine	HY04	HY07	HY06
Camera Height above sea	19 m	19 m	19 m
View Direction	S/W	N/E	S/W
Camera pitch	1.5°	5°	11°
View orientation inwards or outwards from wind farm	Inwards	Inwards	Outwards
Focal length	36 mm	15 mm	4.5 mm
Estimated detection distance for bird of 1m wingspan	~1,500 m	~ 650 m	~ 200 m
Estimated detection height for bird of 1m wingspan	~130 m	~140 m	~100 m
Estimated detection space for bird of 1m wingspan	~12,300,000 m^3	~5,000,000 m^3	~1,300,000 m^3

Figure M14 gives a schematic representation of how the field of view changes according to the focal length of the cameras for each viewpoint. A high focal length (“high zoom”) optimises for a large detection distance, allowing for distant birds to be detected, but with the tradeoff of less monitored space in the vicinity of the camera. A low focal length (“low zoom”) yields lower detection distance, but with the benefit of a larger monitored space in the vicinity of the camera, allowing for more close-up birds to be detected.

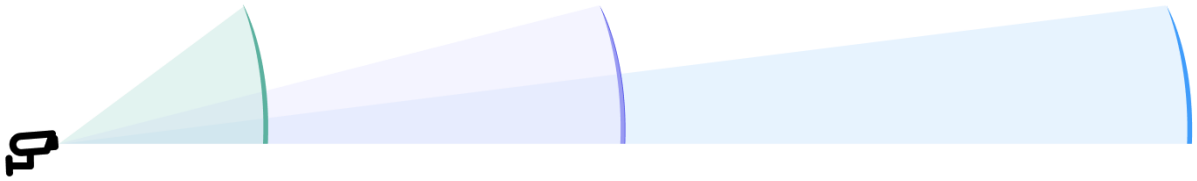

Figure 14: An illustration of the relative detection distances for each viewpoint, determined by the focal length of the cameras. Blue represents viewpoint A with an estimated detection distance of ~1,500 m for a bird of 1 m wingspan, purple represents viewpoint B, and green represents viewpoint C with the corresponding detection distance of ~200 m.

Weather data

Weather data were obtained from a weather station approximately 140 km away on the Norwegian coast. Whilst these data do not offer an exact match for the conditions within the Hywind Tampen Offshore Wind Farm, they are believed to offer a good proxy for those conditions. Data available describe wind speed and direction, precipitation, temperature and a qualitative description of conditions (e.g. clear, cloudy, rain, thunderstorm) on an hourly basis throughout the study period.

Species identification, occurrence, detection distance and tracking duration

Detail on bird detection and tracking, as well as, taxonomic classification procedures are provided in the pilot report[2]. Note, that results concerning species observations, occurrence, detection distance from the cameras, as well as, tracking durations are based on all bird observations made during the 2023-2024 survey period, hereafter referred to as the "full dataset". In addition to differences between viewpoints and in relation to weather conditions, we consider monthly and seasonal patterns in abundance and flight direction. For the purposes of this report, we define seasons as winter (December, January, February), spring (March, April, May), summer (June, July, August) and autumn (September, October, November), roughly reflecting the timing of the annual cycles of many of the species present (spring & autumn migrations, breeding season and winter) (Snow & Perrins 1998).

Data normalisation for interannual comparisons

Birds are known to not be randomly distributed with respect to height above sea level (Johnston *et al.* 2014) and distance from turbines (Johnston *et al.* 2022; Pollock *et al.* 2024). Consequently, variability in the camera settings, ranges and orientations per viewpoint (Table M1), may introduce bias into the data when comparing between cameras (e.g., during interannual comparisons). The

[2] Pilot Report Spoor - AI Avian Monitoring with CCTV Cameras on Floating Wind Turbines Experiences and Future Potential Available online at: https://cdn.equinor.com/files/h61q9gi9/global/26cc50b23fe8e28e10f9cc74c2dad1d20dae188a.pdf?pilot-report-avian-monitoring-on-floating-wind-turbines-2024-equinor.pdf

number of birds recorded is influenced by the maximum detection volume offered by the cameras. This varies according to both the technical specifications of the cameras used, for example focal length and scene width, the environmental conditions in which data are collected, for example visibility, and the size of the species detected, with larger species detected over greater distances, and hence having a greater detection volume, than smaller bodied species. Consequently, for meaningful comparisons between data collected using different approaches (e.g. using buoy-mounted cameras pre-construction and turbine mounted CCTV cameras post-construction) and different locations, data normalization is important to obtain standardized and inter-comparable metrics.

Table M2 summarises the pros and cons for different data normalisation options relating to bird observations. Number of birds/sampling volume/unit time was considered the optimal normalisation option for the data collected at Hywind Tampen as it was important to obtain an understanding of bird abundance (hereafter referred to as the "normalised dataset").

Table M2: Summary of pros and cons of different approaches to normalising bird observation data at Hywind Tampen. Where relevant, alignment with feedback received from the Norwegian Institute for Nature (NINA) is also indicated

Normalisation Options	Pros	Cons	Status
Number of birds observed	Simple and easy to calculate	Does not consider the area covered by the video footage (sampling volume) or the duration of sampling (both attributes of sampling effort), hence, not suitable for comparisons	Not recommended
Number of birds/sampling volume	Accounts for differences in the spatial scale of observations. Useful for density estimates.	Does not consider time / duration of sampling, hence, not suitable for year-year comparisons or within-year comparisons for cameras with different recording times	Not recommended
Number of birds/sampling volume/unit time	Normalizes for both spatial (sampling volume) and temporal (time) scales. Provides a consistent measure for comparing across annual surveys and cameras.	Assumes uniform detectability of birds throughout the volume and time. Does not provide information on bird behaviour.	Recommended
Bird minutes/sampling volume	Incorporates a measure of time that birds spend within the sampling volume, giving a proxy for seabird activity or residency.	Does not consider time / duration of sampling, hence, not suitable for year-year comparisons or within-year comparisons for cameras with different recording times	Not recommended
Bird minutes/sampling volume/unit time	Normalises for both spatial (volume) and temporal time scales, and provides a proxy for bird activity or residency.	Assumes uniform detectability of birds throughout the volume and time. Computationally more complex than number of birds/sampling volume/unit time.	Not recommended
Distance travelled/sampling volume	Useful if the focus is on movement or migratory behaviour rather than presence.	Does consider time / duration of sampling, or bird numbers.	Out of scope
Distance travelled/sampling volume/unit time	Combines spatial, temporal, and movement data, suitable for studies focusing on movement rates or flux through a volume.	Does not consider bird numbers. Distance covered is a weaker proxy to bird activity or residency as it the rate of distance covered will vary by species.	Out of scope

Considering the above, in this report, we normalised bird observations by time and sampling volume. For time, we considered the total of hours recorded during the sampling period. However, as species are likely to be unevenly distributed in space in relation to the turbines on which the cameras are mounted, an additional normalisation step was required to limit analyses to observations made within a similar detection space, hereafter referred to as equal detection space. Since Viewpoint C was the one with shortest estimated detection distance (200 m) this was used to estimate the other dimensions (detection height and width) of the common detection space across all Viewpoints, which resulted in ~31 m and 17.5 m for detection width and height, respectively. Due to the very different detection space characteristics of each camera, the resulting volume of the equal detection space was very small, and captured <3 % of all bird observations. To allow for meaningful comparisons to be made, a pragmatic decision was taken to increase the detection distance to 350 m, which matches the detection distances of actual bird observations made during this survey period by Viewpoint C (see Figure R1). The higher minimum detection distance, resulted in estimates of 54 m and 31 m for detection width and height, respectively. The updated equal detection space led to ~30 % of all bird observations being considered, hereafter referred to as “reduced dataset”.

Impact of weather on abundance

Natural variability (e.g., in response to environmental conditions, diurnal patterns, seasonality etc.) is likely to contribute to uncertainty associated with the numbers and flight directions of birds recorded. To investigate the factors influencing the number of birds recorded, generalized additive models (GAMs) were used to analyse both the normalised dataset and the reduced dataset. This approach highlights the strength and direction of relationships between environmental parameters (see below) and bird abundance, and the uncertainty associated with these estimates. Ultimately, it provides better insights into the contribution of environmental variability to uncertainty associated with data recorded using turbine-mounted CCTV cameras. The environmental parameters included in the GAMs included are presented in Table M3. By analysing both the normalised dataset and the reduced dataset, we aim to demonstrate the value of ensuring data used for analyses are comparable. For the purposes of these analyses bird abundance was standardised by survey effort (i.e., recording times) first, and then aggregated per day. Note, that weather data was not available for 201 out of 2,197 bird observations, which were removed prior to running the GAMs.

Table M3. Environmental parameters used in the GAMs.

Environmental Parameter	Data Source	Method of aggregation	Dataset
Temperature	Norwegian Centre for Climate Services	Average daily	Normalized & Reduced
Wind Speed	Norwegian Centre for Climate Services	Average daily	Normalized & Reduced
Wind Direction	Norwegian Centre for Climate Services	Average daily	Normalized & Reduced
Weather Condition	Norwegian Centre for Climate Services	Most common weather condition day	Normalized & Reduced
Year	This report	N/A	Normalized & Reduced

Month	This report	N/A	Normalized & Reduced

Uncertainty associated with distance, flight heights and flight direction

In addition to the uncertainty introduced into estimates of abundance as a result of the natural variability outlined above, uncertainty will be introduced into estimates of distance, flight heights and flight direction due to error and bias associated with the assumptions underpinning these estimates. These were examined in more detail using the full dataset and following the approach described below.

Error associated with estimates of distance and flight height derived based on bird size

The distance between the camera and the bird, and flight height of the bird are estimated using Spoor's algorithm as follows:

Equation 1 $$\begin{bmatrix} x\_cam \\ y\_cam \\ z\_cam \end{bmatrix} = s \times A^{-1} \times \begin{bmatrix} x\_image \\ y\_image \\ 1 \end{bmatrix}$$

Where, *x_image* is the horizontal distance from the centre of the image in pixels, *y_image* is the vertical distance from the centre of the image in pixels, *s* is the scale factor, *A* is the camera intrinsic matrix, *x_cam* is the horizontal distance of the bird from the centre of the image in meters, *y_cam* is the height of the bird above the camera in meters and *z_cam* is the distance between the bird and the camera in meters.

The camera intrinsic matrix, *A*, is defined as follows:

Equation 2 $$A = \begin{bmatrix} f_x & 0 & c_x \\ 0 & f_y & c_y \\ 0 & 0 & 1 \end{bmatrix}$$

Where, *f* is the focal distance in pixels, and c is the camera principal point.

The scale factor, *s*, is estimated by:

Equation 3 $$s = \frac{obj_{real}}{x_{unscaled}}$$

Where, obj_{real}, is the real world size of the object in millimetres, in this case the wingspan of the bird concerned, assumed to be a standard 1 m, and $x_{unscaled}$ is the size of the object in the image in pixels.

Following Equation 1, estimates of both the flight height of the bird, and the distance of the camera will be influenced by the scale factor, *s*, which is dependent on the estimated real world size of the bird (Equation 3). Consequently, error was introduced into estimates of both distance and flight height as a consequence of natural variability in bird body size (Boersch-Supan *et al.* 2024).

Following Boersch-Supan *et al.* (2024), a Monte Carlo simulation approach was used, resampling bird wingspans from known distributions (Table M4) in order to recalculate distance from the camera and flight heights, by substituting these values into Eq. 3, above. Values for $x_{unscaled}$ were based on the first observation of each bird in the full dataset. This gave an indication of the potential error introduced into these metrics through assumptions about bird body size. Data from the most commonly observed species were considered in this analysis.

Table M4 Wingspans used when estimating species flight heights and distance from camera.

	Wingspan
Unidentified Gulls	Randomly sampled from distributions for Herring Gull, Great Black-backed Gull and Kittiwake
Herring Gull	1.44 m (SD 0.0300)[1]
Great Black-backed Gull	1.58 m (SD 0.0375)[1]
Kittiwake	1.08 m (SD 0.0625)[1]
Fulmar	1.07 m (SD 0.0150)[2]
Gannet	1.72 m (SD 0.0375)[1]

[1]https://www.nature.scot/doc/guidance-note-7-guidance-support-offshore-wind-applications-marine-ornithology-advice-assessing#appendix-1-interim-recommended-parameters-by-species.[2]Snow & Perrins (1998) The Birds of the Western Palearctic Concise Edition. Volume 1. Oxford University Press.

Flight direction

Flight direction was estimated based on a comparison between the first and last point detected for each bird, drawing from the full dataset. This approach overlooks any potential uncertainty in flight directions that will be present if birds are not engaged in directed flight (e.g. are not on migration, or are not commuting between breeding colonies and foraging areas). This uncertainty was quantified for each track by randomly sampling points and estimating the flight direction between them. Following a Monte Carlo simulation approach, this sampling was repeated over 1000 iterations for each track and the mean and standard deviations of these were estimated across all iterations, taking the circular nature of cardinal directions into account. This analysis gave an indication of the potential error introduced into estimates of flight directions based on a comparison of the first and last points of each track.

Uncertainty was also introduced into estimates of flight direction by natural variability in the data. For example, the potential for flight directions to vary between years, species, seasons and viewpoints. Comparisons were made between flight directions estimated according to each of

these factors, giving an indication of the potential uncertainty introduced into estimates of flight direction as a consequence of natural variability.

Testing reduced file size

As an experiment, to test the possibility of reducing the file size of video recordings and thereby the storage requirements, videos recorded during December 2024 and January to February 2025 had their frame rates lowered from 30 frames per second (FPS) to 10 FPS and analysed for bird activity. It was expected that the effect of reducing the framerate would have some effect on the quality of the results and the ability of the system to detect and track birds, but this effect was not expected to be significant or impact the results to a large extent. The analysis performed here was ultimately limited to the videos recording during December 2024, as this was deemed sufficient, and processing and analysing the remaining videos from January and February wouldn't add more value to the results of the experiment.

Results

Data capture

Birds observed in relation to detection distance, detection height, and detection width per Viewpoint are shown in Figure R1. In all cases, birds were observed further away than the theoretical maximum detection limit across all dimensions. The theoretical maximum detection distance is based on a minimum density of 8 pixels per meter. However, in this instance, particularly in the case of the larger species present at this site, data could be obtained at lower pixel densities.

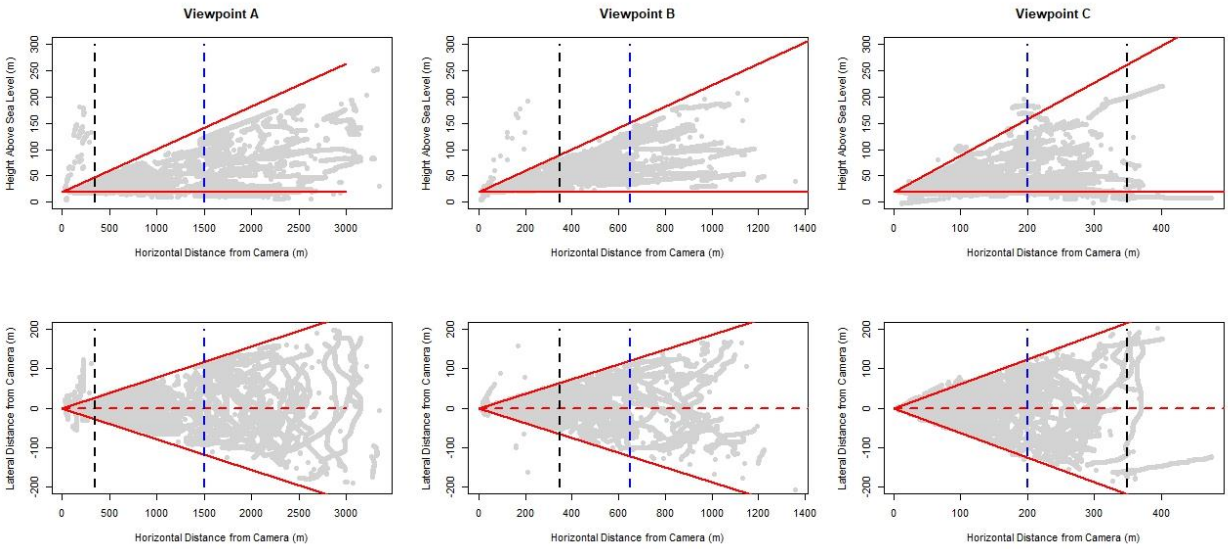

Figure R1. Bird observations in relation to vertical (top) and horizontal (bottom) field of view for each camera. Red lines indicate field of view, blue lines indicate theoretical maximum detection distance for a bird with a 1 m wingspan,

black line indicates the extent used when standardising data between cameras, whilst this is beyond the theoretical maximum detection distance for Viewpoint C, this was a pragmatic choice to maximise the data included when standardising between cameras, reflecting the fact that a substantial number of birds were recorded at distances of 350 m from Viewpoint C. This is likely to be due in part to the fact that the typical wingspan of many species recorded on the site (e.g. large gulls, Northern Gannet) exceeds 1 m.

Bird observations at Hywind Tampen

Species

A total of 16 bird taxa were identified across 2023-2024 (full dataset), 11 at the species level, 1 at the family level, 2 at the Order level, 1 at the Clade level, 1 at the Class level (Figure R2; Appendix Table 1). Total number of bird observations across viewpoint were 756, 563, and 878 for Viewpoints A, B, and C, respectively (Figure R2; Appendix Table 1). Additional detail on observation per species and viewpoint is available in Appendix Table 1. Bird observations across season are available in Table R1. As might be expected from previous studies, there were seasonal and annual patterns in species abundance (e.g. Robertson *et al.* 2014; Warwick-Evans *et al.* 2016), with fewer birds detected in 2024 than were detected in 2023. A key contributor to these differences appears to be the greater number of gulls (both Great Black-backed Gulls and unidentified gulls) detected during autumn migration in 2023 than in 2024 (Figure R3).

The most commonly observed and identified species was the Great Black-backed Gull. A substantial proportion of the unidentified gulls are also likely to be Great Black-backed Gulls, though imagery was not clear enough to allow positive identification. Great Black-backed Gulls have a complex migratory strategy (Anker-Nilssen *et al.* 2000). The population is partially migratory, and whilst many individuals may remain in Norway throughout the year, others move in a south-westerly direction following the end of the breeding season, wintering in the United Kingdom, and elsewhere in Europe (Robinson *et al.* 2024). This is reflected in records of the species within Hywind Tampen throughout the year. The remaining species are mostly either breeding seabirds which may occur in and around the site whilst foraging (Northern Gannet, European Herring Gull, Northern Fulmar, Black-legged Kittiwake, Great Skua) and/or when migrating between breeding and wintering locations, and passage migrants detected during spring or autumn migration (Barn Swallow, White Wagtail and other small passerines, Short-eared owl, raptors and waders). The exceptions to this are European Shag/Great Cormorant, which were only recorded during winter, when they may take advantage of opportunities to roost on the turbine structures, and great spotted woodpecker, a species which does not typically undertake substantial movements or migrations except as juvenile or immature birds (Snow & Perrins 1998).

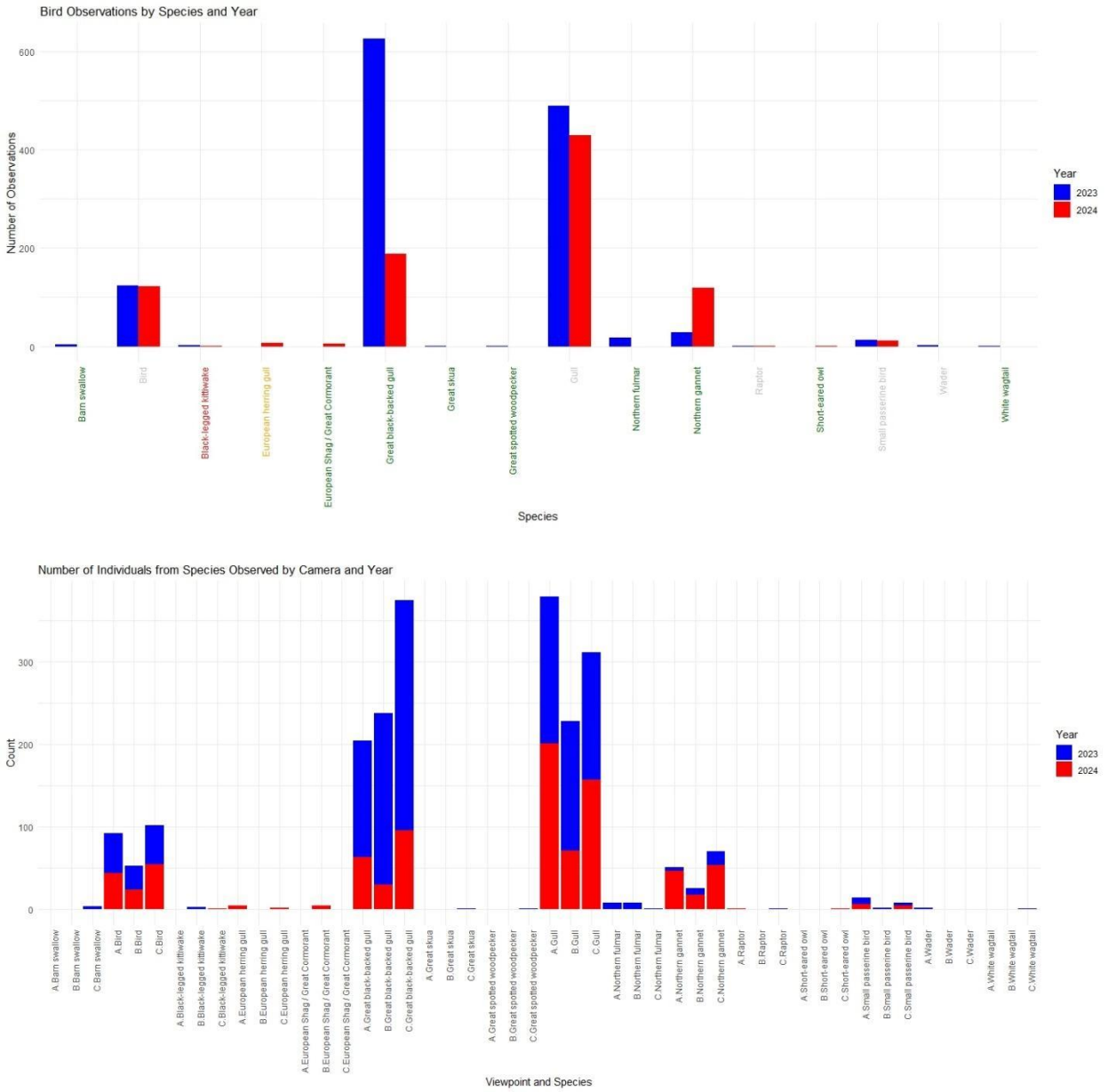

Figure R2. Top: Number of individuals from each species/group observed by year, label colours on the x-axis indicate Norwegian Red List status for each species – Endangered, Vulnerable, Least Concern, Not Applicable (e.g., a group rather than individual species). Bottom: Number of individuals from each species/group observed by year and Viewpoint.

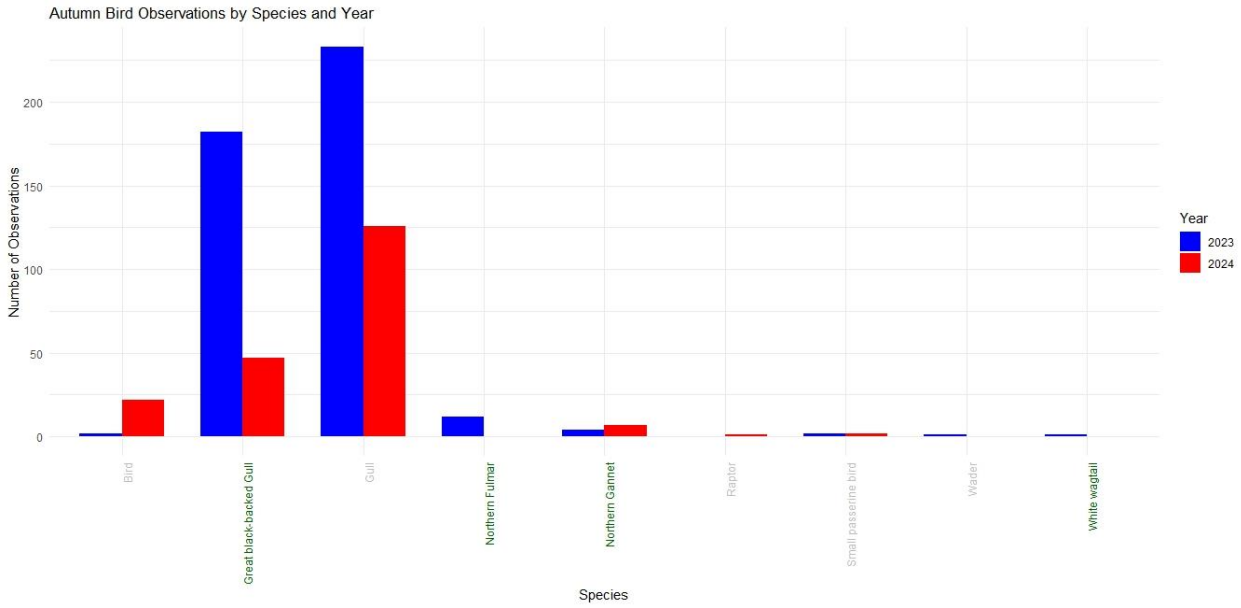

Figure R3. Number of individuals from each species/group observed during autumn migration by year, label colours on the x-axis indicate Norwegian Red List status for each species – Endangered, Vulnerable, Least Concern, Not Applicable (e.g., a group rather than individual species).

Table R1. Number of individuals from each species/group observed by season considering all birds observations (full dataset) during May 2023-November 2024.

Common Name (Taxon Name)	Status	Autumn	Spring	Summer	Winter
Barn swallow (*Hirundo rustica*)	Passage migrant	0	4	0	0
Bird (Aves)	NA	67	39	94	47
Black-legged kittiwake (*Rissa tridactyla*)	Breeding	0	0	4	0
European herring gull (*Larus argentatus*)	Breeding	0	5	1	1
European Shag / Great Cormorant (*Phalacrocorax aristotelis / Phalacrocorax carbo*)	Wintering	0	0	0	5
Great black-backed gull (*Larus marinus*)	Partial migrant	229	48	457	82
Great skua (*Stercorarius skua*)	Breeding	0	0	1	0
Great spotted woodpecker (*Dendrocopos major*)	Vagrant	0	0	1	0
Gull (Laridae)	Partial migrant	359	111	285	163
Northern fulmar (*Fulmarus glacialis*)	Breeding	12	0	5	0
Northern gannet (*Morus bassanus*)	Breeding	11	59	70	7
Raptor	Passage migrant	1	0	1	0
Short-eared owl (*Asio flammeus*)	Passage migrant	0	1	0	0

Small passerine bird (Passeriformes)	Passage migrant	4	8	11	1
Wader (Charadriiformes)	Passage migrant	1	0	1	0
White wagtail (*Motacilla alba*)	Passage migrant	1	0	0	0
Total number of species observed		**4**	**5**	**7**	**4**
Total number of species / groups observed		**9**	**8**	**12**	**7**

Detection distances and tracking durations

Analysis of the overall minimum and maximum detection distances for birds observed, using the full dataset, provides insights on the actual capabilities of the camera setup. Results are most informative for groups with larger numbers of detections; for example, Great black-backed gull. In general, the trends are similar between species/groups and show that most birds are detected closer to the cameras (within the first ~100 m) as opposed to further away (Figure R4); however, smaller numbers of first detections are made out to 1000s of metres (Figure R5). In terms of the maximum detection distances for birds recorded, those unidentified birds with coarse groupings (e.g., birds / gulls), are detected at a greater distance compared to species-level groupings with the exception of the Great black-backed gull and a small passerine bird (Figure R5). The camera at Viewpoint A, which had the longest detection capability, detecting birds over greater distances (mean minimum detection distance of 888 m ± 720 m standard deviation across all observations), followed by Viewpoint B (351 m ± 277 m), and lastly Viewpoint C (105 m ± 84) with the shortest detection capability.

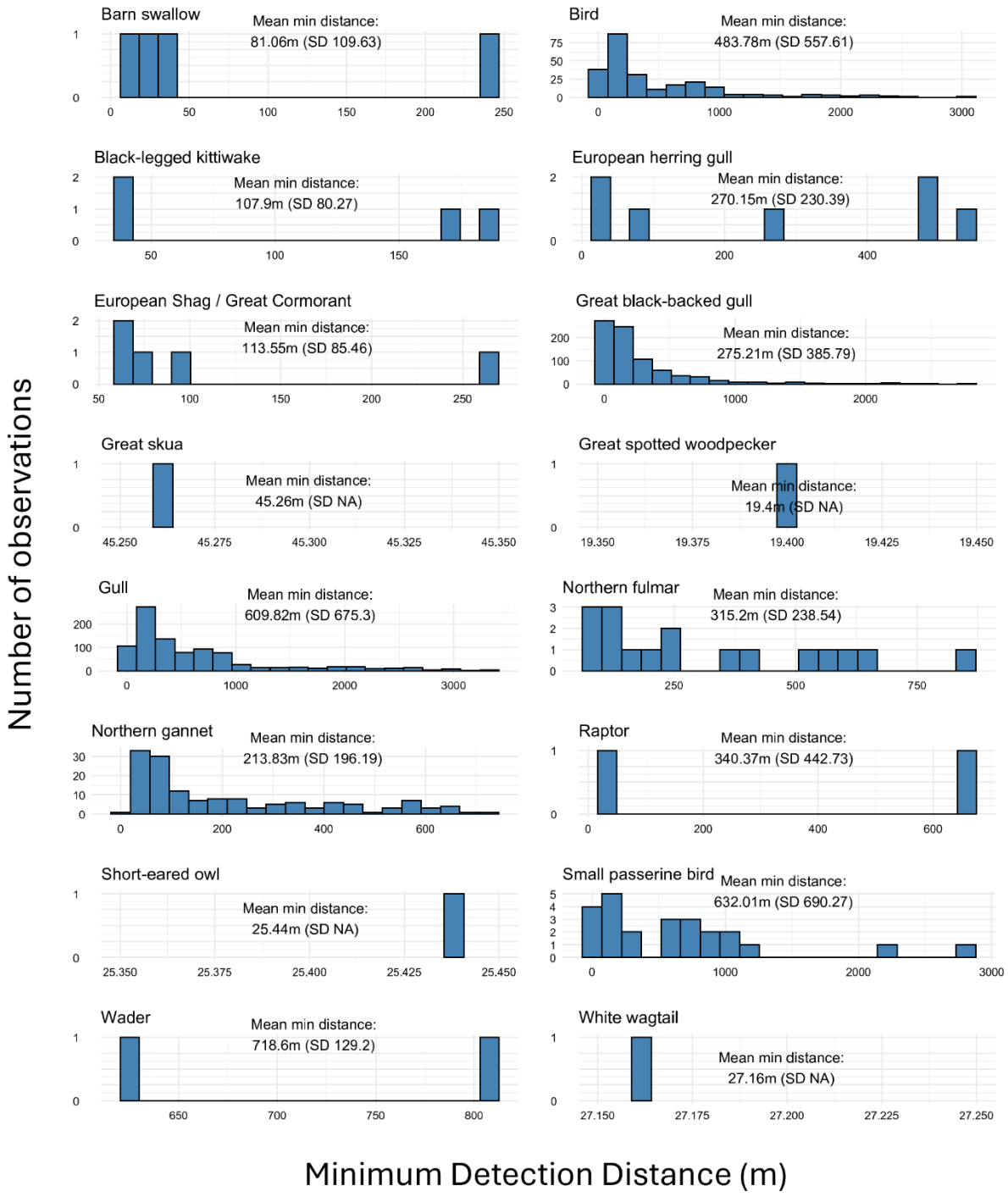

Figure R4: Minimum detection distances at which bird species/groups were detected across all viewpoints combined throughout 2023-2024.

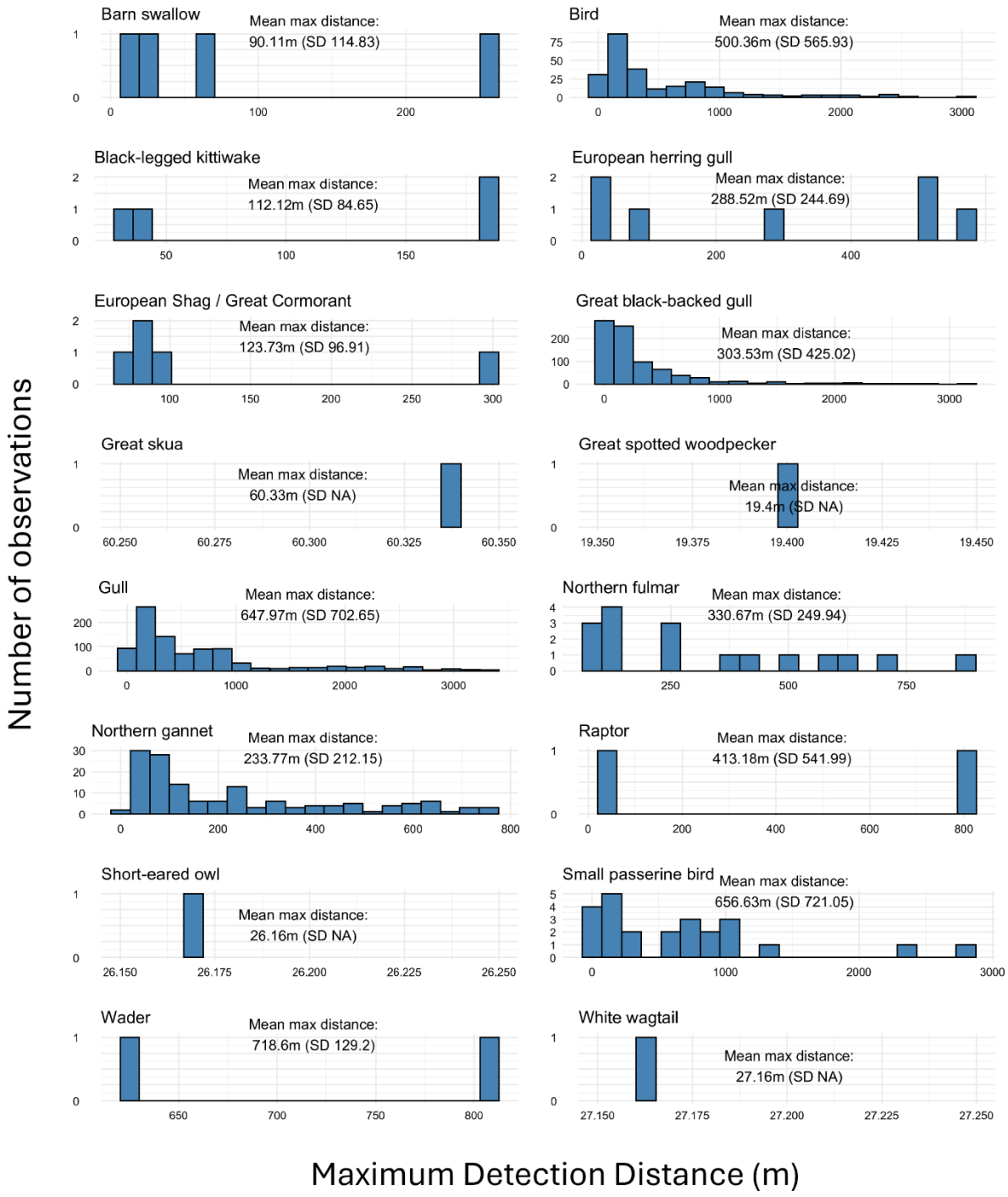

Figure R5: Maximum detection distances at which bird species/groups were detected across all viewpoints combined throughout 2023-2024.

Tracking duration varied between ~8-10 seconds for the most commonly observed birds such as the Great black-backed gull and other gulls (Figure R6; Table R1). Average tracking duration was broadly similar between cameras, except for some including Northern Fulmar, and, small passerine birds, however, these had few observations overall (10 and 24, respectively).

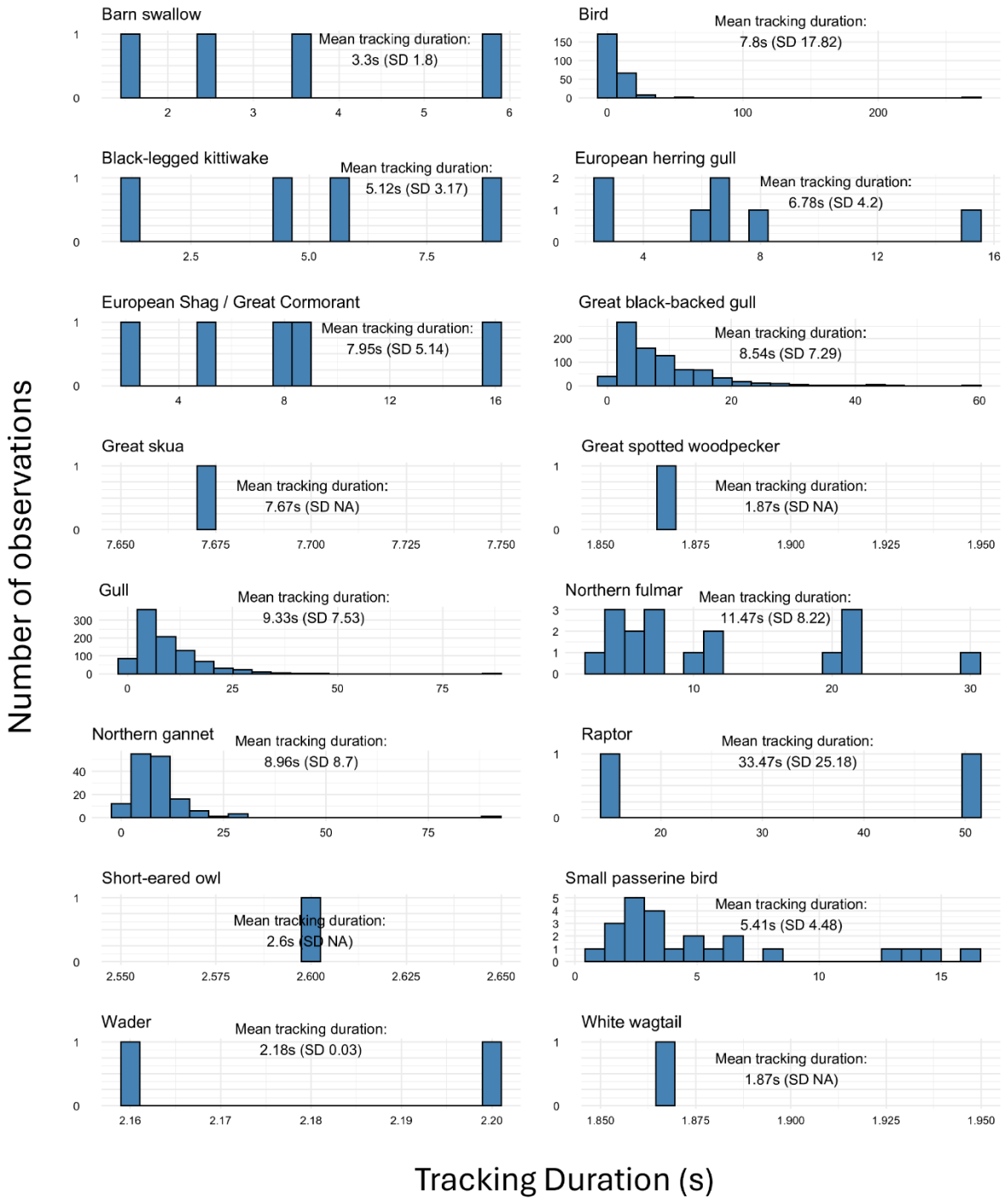

Figure R6: Tracking durations of bird species/groups across all viewpoints combined throughout 2023-2024.

Impact of weather conditions

Table R2 indicates the impact of weather conditions on the bird minimum and maximum detection distances, and the bird tracking durations from the full dataset. As might be expected, detection

distances were significantly lower during foggy conditions, but comparable during clear, cloudy and rainy conditions (Figure R7). Tracking durations seemed to be comparable across weather conditions (Figure R7).

Table R2: Mean minimum and maximum detection distances, and tracking durations across all bird observations (full dataset) under different weather conditions. Weather conditions were grouped to four categories for statistical comparisons.

Weather condition	**Weather category group**	**Minimum distance (m)**		**Maximum distance (m)**		**Tracking duration (s)**		**Total observations per weather condition**
		Mean	**Sd**	**Mean**	**Sd**	**Mean**	**Sd**	
Clear	Clear	457.74	710.83	480.85	723.02	8.44	7.20	75
Fair		485.63	663.97	504.49	675.76	7.79	6.63	91
Cloudy	Cloudy	430.27	563.61	462.06	595.30	8.82	9.78	1540
Fog	Fog	200.29	264.62	215.48	285.45	6.76	5.40	29
Light Rain	Rain	450.38	624.37	487.95	661.98	9.68	8.15	125
Rain Shower		172.81		188.67		5.53		1
Rain		528.12	667.13	553.29	678.22	10.51	12.18	104
Heavy Rain		406.23	617.87	428.32	630.12	8.89	8.32	27
Light Snowfall		247.59	149.12	248.31	148.56	4.98	3.11	4
NO weather data	N/A	452.68	309.61	480.66	319.15	8.11	6.16	201

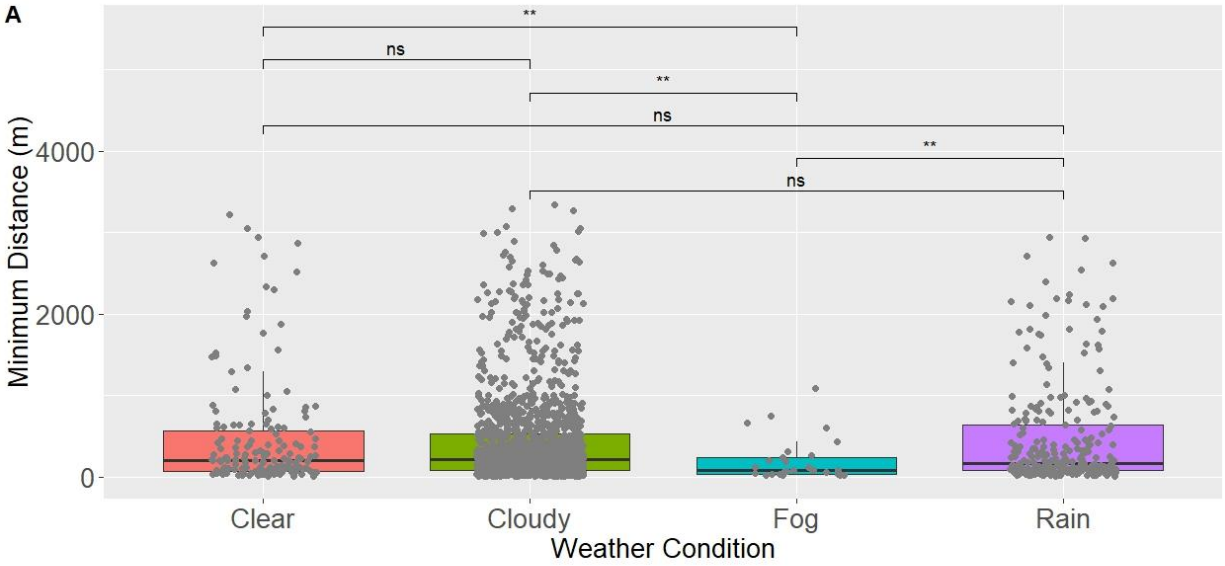
A
Minimum Distance (m)
0
2000
4000
**
ns
**
ns
**
ns
Clear
Cloudy
Fog
Rain
Weather Condition

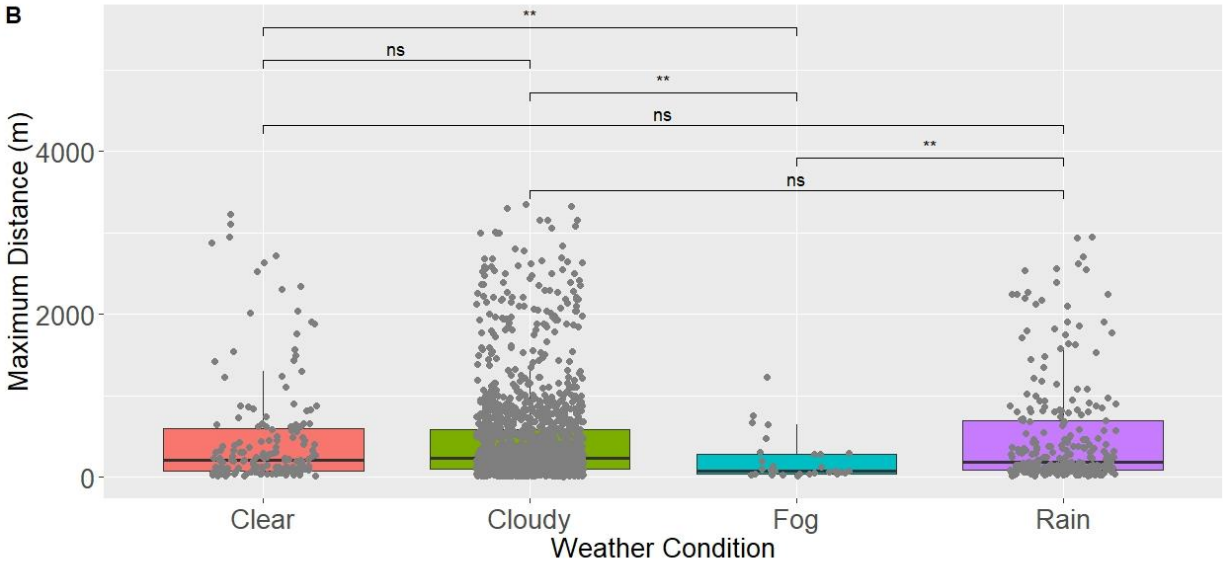
B
Maximum Distance (m)
0
2000
4000
**
ns
**
ns
**
ns
Clear
Cloudy
Fog
Rain
Weather Condition

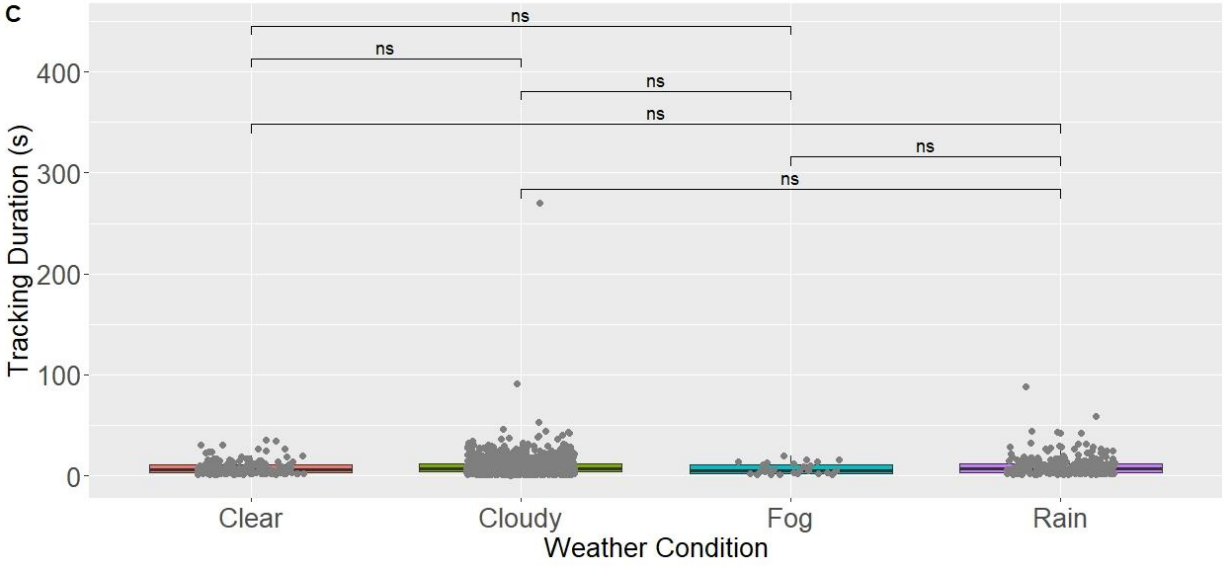
C
Tracking Duration (s)
0
100
200
300
400
ns
ns
ns
ns
ns
ns
Clear
Cloudy
Fog
Rain
Weather Condition

Figure R7: Minimum and maximum detection distances, and tracking duration at which birds were detected in relation to prevailing weather conditions. "Light rain", "Rain showers", "Heavy Rain", and "Light Snowfall" categories were grouped under Rain, and "Fair" was grouped with "Clear". A total of 201 bird observations with no associated weather condition information were removed from this plot. Boxes indicate median, and the 25th and 75th quantiles, whiskers are 1.5 times the interquartile. Asterisks indicate significant differences as identified by the pairwise Wilcoxon Rank-Sum test, adjusted for multiple comparisons using the False Discovery Rate (FDR) method (Benjamini-Hochberg correction). Significance levels = 0.05 (*), 0.01 (**) level, respectively; ns = not significant.

Analysis of abundance

Two GAMs were used to investigate the effect of environmental parameters, using the normalised and reduced datasets. Both GAMs indicate a significant decline in total abundance in 2024, with strong negative effects in both the normalized and reduced datasets (Tables R3 and R4). In the normalised dataset, wind speed is the only significant predictor ($p < 0.05$; Table R3) indicating a negative relationship in bird abundance with increasing wind speed (Figure R8). Whereas in the reduced dataset, month is significant ($p < 0.05$, Table R4) indicating higher abundances around the summer period (Figure R9). Weather conditions are not significant in either model. The reduced dataset explains more deviance (52.8% vs. 45.3%) and has a lower GCV (0.79 vs. 0.95), indicating slightly better predictive performance, though its adjusted R^2 is lower indicating that it captures less variability.

Table R3. Summary of the Generalized Additive Model (GAM) fit based on the normalized dataset, displaying estimated model coefficients, standard errors, test statistics, and significance levels. The table includes both parametric coefficients and smooth terms, where the effective degrees of freedom (edf) reflect the complexity of the smooth functions. The significance of smooth terms is assessed using approximate F-statistics. Additional model diagnostics include the percentage of deviance explained, the generalized cross-validation (GCV) score, and the R-squared value, which provide insights into model fit and predictive performance. Lower GCV scores and higher R-squared values indicate better model performance.

Normalized dataset GAM					
Model formula: Total_Abundance ~ s(Avg_Temperature) + s(Avg_WindSpeed) + s(Avg_WindDirection) + Most_Common_Weather + Year + s(Month, bs = "re") Family: Gamma; Link function: log					
Parametric coefficients:	**Estimate**	**Std. Error**	**t value**	**Pr(>|t|)**	**Sig.**
(Intercept)	1.0162	0.2355	4.316	2.5e-05	***
Most_Common_WeatherCloudy	0.1586	0.6455	0.669	0.504	
Most_Common_WeatherFog	0.5541	0.6115	0.858	0.392	
Most_Common_WeatherRain	0.3089	0.3292	0.938	0.349	
Year2024	-1.042	0.1401	-7.448	<2e-16	***
Approximate significance of smooth terms	**Edf**	**Ref.df**	**F**	**p-value**	**Sig.**
s(Avg_Temperature)	2.22586	2.850	1.381	0.189	
s(Avg_WindSpeed)	8.26022	8.841	7.079	<2e-16	***
s(Avg_WindDirection)	1.00048	1.001	0.5	0.481	
s(Month)	0.00675	8	0.001	0.410	
*Sig. codes: 0 '***', 0.001 '**', 0.01 '*', 0.05 '.', 0.1 ' ', 1*					
R-sq.(adj) = 0.206, Deviance explained = 45.3%, GCV = 0. 95116, Scale est. = 0.93097, n = 216.					

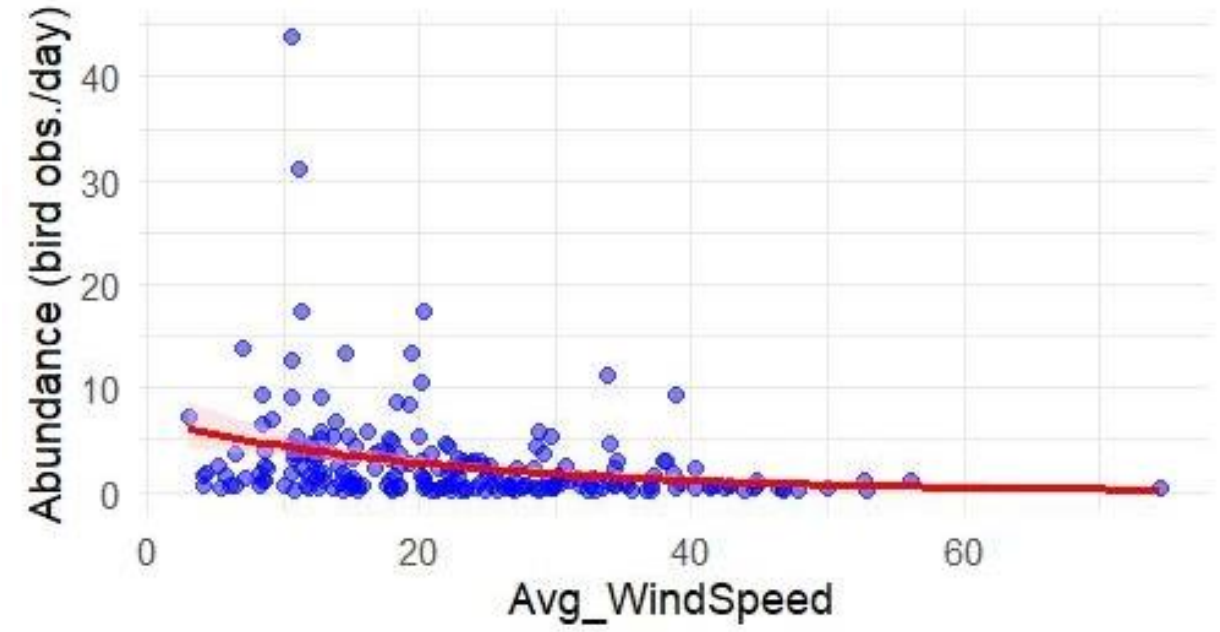

Figure R8. Relationship between abundance (bird observations per day) and wind speed used as per the normalizedl dataset GAM. Scatter plots show the observed abundance data points (blue), with the smooth effect of wind speed on abundance indicated by the red line and shaded area. The red line represents the estimated GAM smoother, and the shaded area represents the 95% confidence interval.

Table R4. Summary of the Generalized Additive Model (GAM) fit based on the reduced dataset, displaying estimated model coefficients, standard errors, test statistics, and significance levels. The table includes both parametric coefficients and smooth terms, where the effective degrees of freedom (edf) reflect the complexity of the smooth functions. The significance of smooth terms is assessed using approximate F-statistics. Additional model diagnostics include the percentage of deviance explained, the generalized cross-validation (GCV) score, and the R-squared value, which provide insights into model fit and predictive performance. Lower GCV scores and higher R-squared values indicate better model performance.

Reduced dataset GAM					
Model formula: Total_Abundance ~ s(Avg_Temperature) + s(Avg_WindSpeed) + s(Avg_WindDirection) + Most_Common_Weather + Year + s(Month, bs = "re") Family: Gamma; Link function: log					
Parametric coefficients:	**Estimate**	**Std. Error**	**t value**	**Pr(>|t|)**	**Sig.**
(Intercept)	-6.1156	0.4082	-14.981	< 2e-16	***
Most_Common_WeatherCloudy	-0.2093	0.3527	-0.593	0.554	
Most_Common_WeatherFog	-0.3916	0.5706	-0.686	0.494	
Most_Common_WeatherRain	-0.2561	0.423	-0.605	0.546	
Year2024	-1.2677	0.1911	-6.633	1.14E-09	***
Approximate significance of smooth terms:	**Edf**	**Ref.df**	**F**	**p-value**	**Sig.**
s(Avg_Temperature)	1.743	2.179	1.129	0.293677	
s(Avg_WindSpeed)	1	1	1.724	0.191807	
s(Avg_WindDirection)	6.729	7.814	1.198	0.27466	
s(Month)	6.145	8	3.331	0.000124	***
*Sig. codes: 0 '***', 0.001 '**', 0.01 '*', 0.05 '.', 0.1 ' ', 1*					
R-sq.(adj) = 0.0992; Deviance explained = 52.8%, GCV = 0.78487; Scale est. = 0.78411; n = 135					

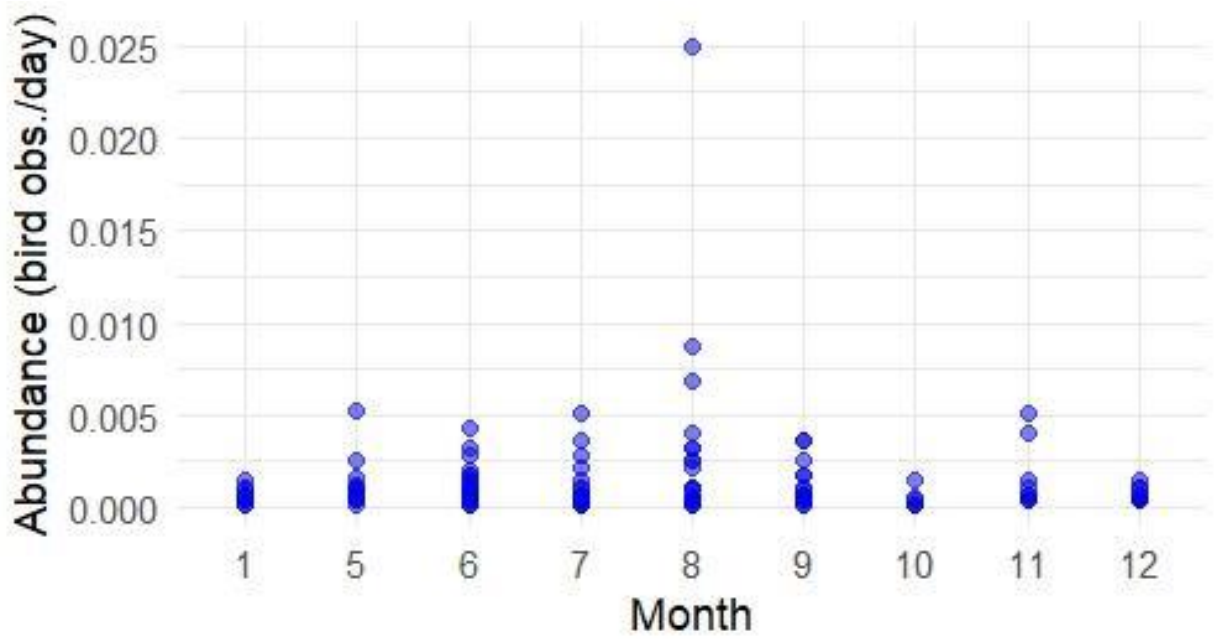

Fig R9. Relationship between abundance (bird observations per day) (blue points) and Month as per the reduced dataset GAM.

Comparison of data between months, seasons and years

Recording duration across month, season and year are available in Appendix Table 2. These were used to normalise abundances for survey effort (= recording duration), which in combination with normalising for detection space, resulted in the reduced dataset. Daily bird abundance from the reduced dataset was comparable across all months, with the exception of February-March where no birds were detected (Figure R10), likely reflective of the seasonal abundance and distribution of the most commonly recorded species – Northern Gannet and Great Black-backed Gull – in the North Sea (Waggitt et al. 2020). Pairwise comparisons did not find significant differences in daily bird abundance between the remaining months (Table R5). No observations in February-March and lower abundances in April was not due to lower survey effort, since recording duration was comparable between November and February (Appendix Table 2). On the other hand, season did not seem to have a significant effect on daily abundance. This is likely to be because whilst summer months typically had the greatest abundance of birds, they also had the greatest within-season variation in abundance, encompassing values present during other seasons, and making it more challenging to distinguish these values statistically (Figure R10). Finally, daily bird abundances were significantly higher in 2023 than 2024 (Figure R10).

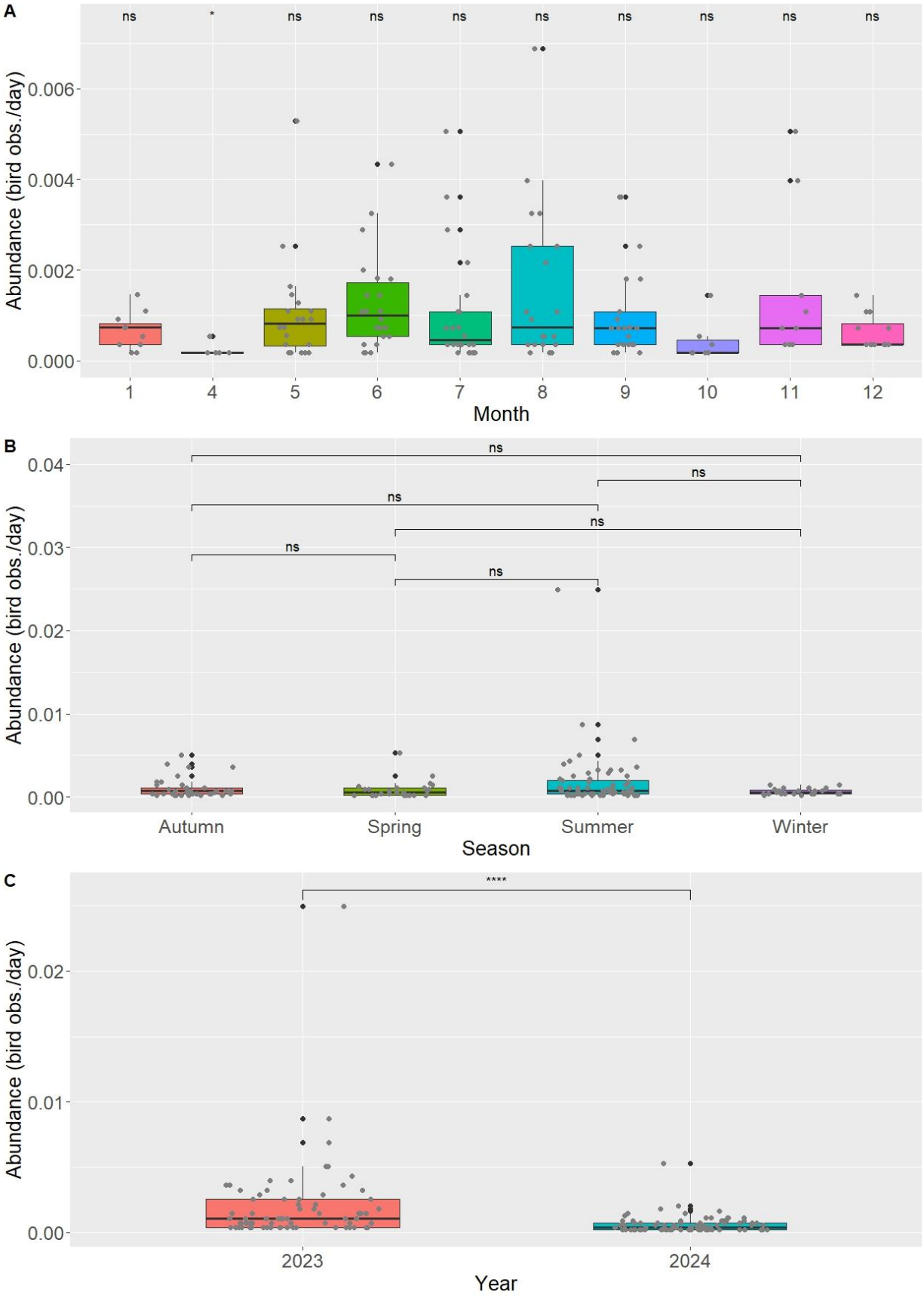
A
ns
*
ns
ns
ns
ns
ns
ns
ns
ns
Abundance (bird obs./day)
0.006
0.004
0.002
0.000
1
4
5
6
7
8
9
10
11
12
Month
B
ns
ns
ns
ns
ns
ns
Abundance (bird obs./day)
0.04
0.03
0.02
0.01
0.00
Autumn
Spring
Summer
Winter
Season
C
****
Abundance (bird obs./day)
0.02
0.01
0.00
2023
2024
Year

Figure R10. Daily abundance across year, season and month. Boxes indicate median, and the 25^{t} and 75th quantiles, whiskers are 1.5 times the interquartile. Asterisks indicate significant differences as identified by the pairwise Wilcoxon Rank-Sum test, adjusted for multiple comparisons using the False Discovery Rate (FDR) method (Benjamini-Hochberg correction). Significance levels = 0.05 (*), 0.01 (**) level, respectively; ns = not significant.

Table R5. Pairwise Wilcoxon Rank-Sum test for differences in daily bird abundance across months. The p-value adjusted using the False Discovery Rate (FDR) method (Benjamini-Hochberg correction), which accounts for multiple comparisons.

Month	January	April	May	June	July	August	September	October	November
April	0.15								
May	0.7	0.15							
June	0.38	0.12	0.57						
July	0.84	0.16	0.72	0.38					
August	0.44	0.12	0.48	0.79	0.32				
September	0.93	0.12	0.89	0.5	0.72	0.48			
October	0.33	0.7	0.29	0.15	0.38	0.15	0.21		
November	0.72	0.12	0.79	0.93	0.5	0.87	0.7	0.19	
December	0.58	0.12	0.57	0.22	0.87	0.22	0.55	0.38	0.38

Species flight heights

The position and pitch of the cameras means that all birds recorded in the full dataset will be well above the sea surface (Table M1 & Figure R1), this bias cannot be addressed through using either the normalised, or reduced datasets. As a consequence, estimates of species mean flight heights (Table R6) will be positively biased, and greater than those reported elsewhere (e.g. Johnston et al. 2014). As would be expected, given that many of the species recorded tend to fly close to the sea surface (Johnston et al. 2014), these mean estimates are close to the lower limit of the field of view of the camera.

Table R6 Mean flight heights of birds recorded from CCTV cameras

Species	Mean Flight Height in meters (Standard Deviation)
Barn swallow	50.42 (53.02)
Unidentified Bird	41.45 (33.31)
Black-legged kittiwake	23.59 (0.98)
European herring gull	26.72 (4.95)
European Shag / Great Cormorant	25.5 (3.4)
Great black-backed gull	34.07 (21.42)
Great skua	15.91*
Great spotted woodpecker	21.21*
Unidentified Gull	54.29 (39.59)
Northern fulmar	32.13 (8.05)
Northern gannet	24.39 (7.06)

Raptor	38.48 (11.66)
Short-eared owl	31.21*
Small passerine bird	50.95 (30.31)
Wader	45.85 (3.28)
White wagtail	24.86*

*Based on a single record

Continuous flight height distributions can be generated for species for which over 100 records are available (Johnston & Cook 2016). Based on the data available continuous flight height distributions were generated for all birds, Great Black-backed Gulls and Northern Gannets (Figure R11). These distributions indicated that over 98% of recorded birds were flying at heights likely to place them at risk of collision. However, the proximity of the lower limit of the camera field of view to the lower limit of the rotor sweep means that these data are strongly biased and do not reflect the true collision risk of species present within the wind farm.

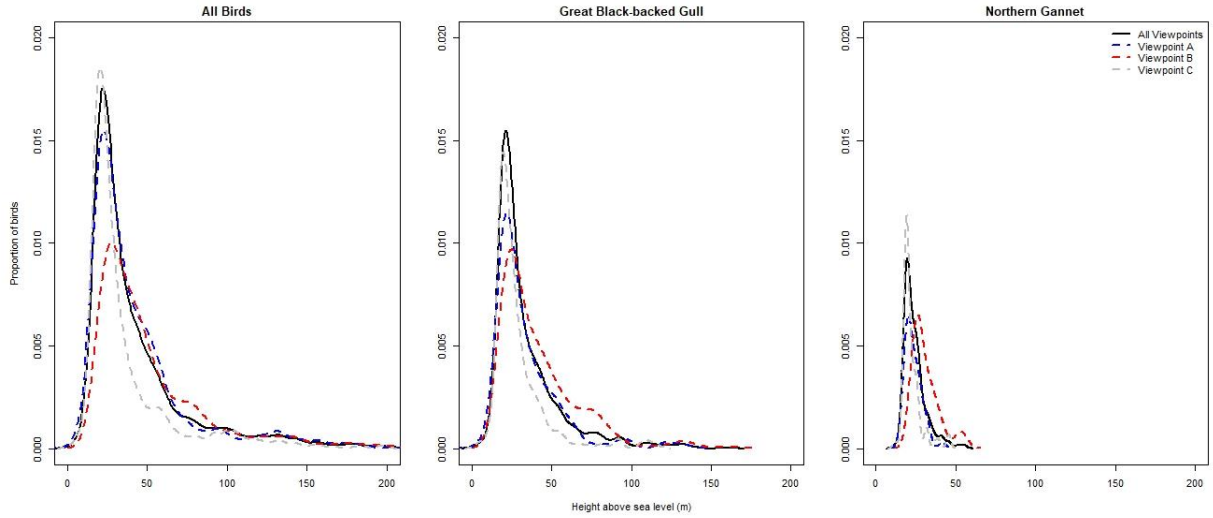

Figure R11 Continuous flight height distributions for all birds, Great Black-backed Gulls and Northern Gannets recorded within the Hywind Tampen Offshore Wind Farm using CCTV cameras.

Estimates of error

Error associated with estimates of distance and flight height derived based on bird size

As might be expected, assumptions around a standard 1 m wingspan for all species introduced error into estimates of both distance from camera and flight height (Table R7). This error was more substantial for distance to the camera than for flight height, though, in part, this is likely to reflect the scales over which the two parameters were measured. It should be noted that the errors associated with flight height estimates are of a similar magnitude to those obtained from

tracking data (Johnston *et al.* 2023), and less substantial than those obtained from digital aerial surveys using size-based methodologies (Boersch-Supan *et al.* 2024).

Assumptions around the wingspan influence estimates of the real-world size of the bounding box used to calculate bird position in Eq.'s 1-3, above. Consequently, the errors associated with estimates of distance and flight height are strongly correlated with the wingspan of the species concerned. This means that the error associated with estimates for birds with wingspans closer to 1 m is less than is the case for species which have a wingspan which is much greater than 1 m (Figure R12). However, it should also be noted that these analyses do not take the orientation of the birds into account. For larger species, like gannets, this is likely to mean that the values in Table R7 reflect the maximum possible error. For species such as kittiwake or fulmar, with wingspans which are close to 1 m, changes in orientation are likely to result in a greater discrepancy between the assumed and actual real world sizes of the bounding box.

Table R7. Median Root Mean Squared Error (RMSE) associated with distance from camera and flight heights estimated using a standard 1 m wingspan for all birds versus a wingspan sampled from a known distribution for each species.

	Median RMSE Distance	Median RMSE Flight Height
Unidentified gulls	137.30 m	5.19 m
Gannet	138.51 m	8.76 m
Great black-backed Gull	76.11 m	5.21 m
Herring Gull	53.95 m	0.03 m
Kittiwake	14.90 m	1.15 m
Fulmar	31.37 m	0.70 m

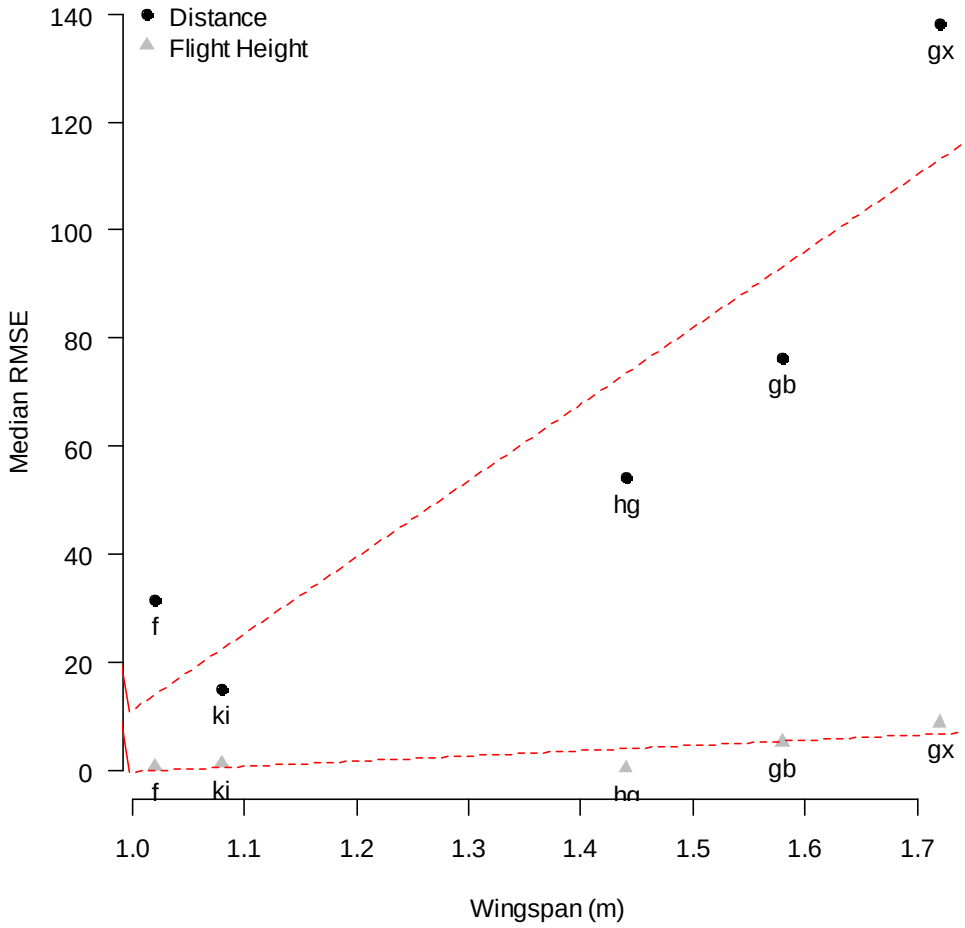

Figure R12. Median Root Mean Squared Error (RMSE) associated with distance from camera and flight heights estimated using a standard 1 m wingspan for all birds versus a wingspan sampled from a known distribution for each species (f = fulmar, ki = kittiwake, hg = herring gull, gb = great black-backed gull, gx = gannet), in relation to the wingspan of the species concerned. Red lines indicate best fit for relationship between wingspan and RMSE.

Direct comparison of points estimated using a wingspan estimate sampled from a known distribution with those assuming a 1 m wingspan estimate indicates that the resultant error is likely to increase with distance from the camera (Figures R13-R15). The variability around the estimates drawn from a known distribution of wingspans varies between species. For species with a greater variability in wingspan, such as larger gulls, there is greater variability in the resultant estimates of distance. This variability is greatest when there is uncertainty around species identification, as is the case for unidentified gulls (Figure R15). However, the magnitude of this variability is typically less than the error introduced through assumptions of a 1 m wingspan. Similar patterns are seen in relation to estimates of flight height (Figures R16–R18), though it is important to note that whilst error around flight height estimates does appear to be correlated with height, it does not appear to be strongly correlated with distance from the camera (Figure R19).

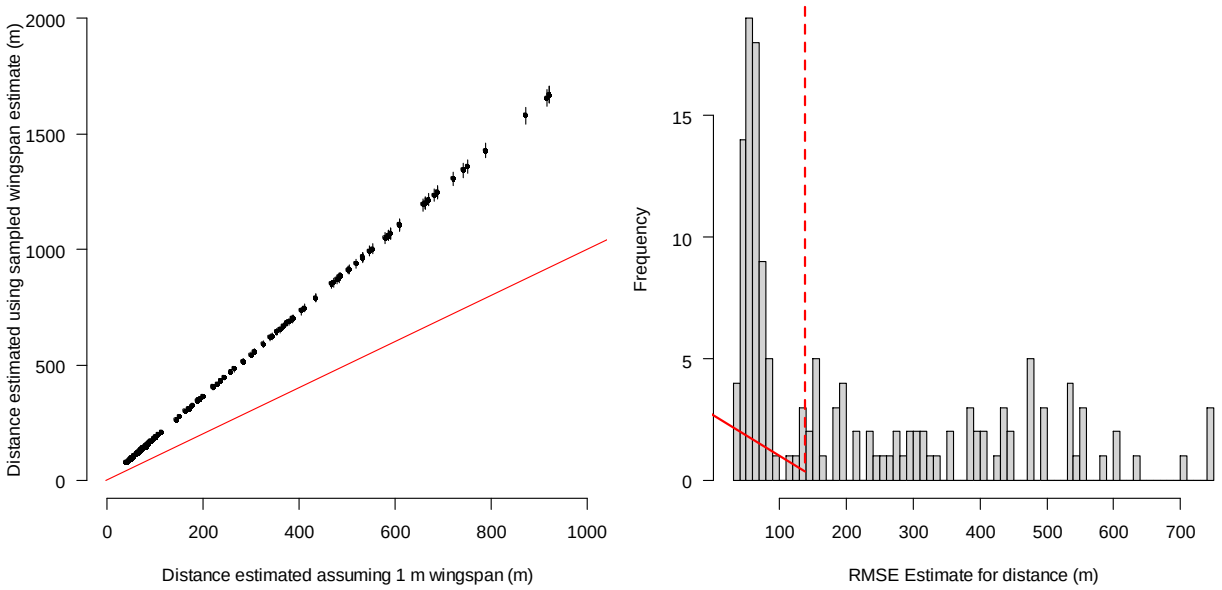

Figure R13. (Left) Distance estimated for gannets using a wingspan estimated sampled from a known distribution in comparison to distance estimated using an assumed 1 m wingspan, red line indicates where points would lie if there were a perfect match between the two. (Right) Distribution of root mean squared error (RMSE) of estimated distance using a sampled wingspan estimate in comparison to an assumed 1 m wingspan, red line indicates median RMSE of 138 m.

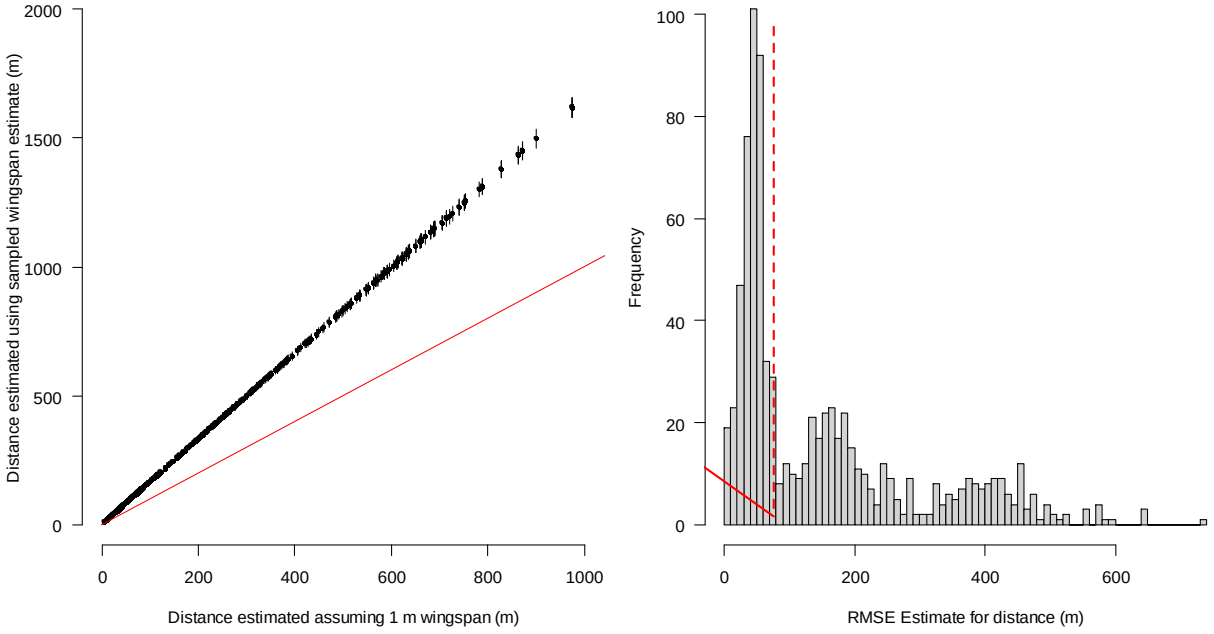

Figure R14. (Left) Distance estimated for great black-backed gulls using a wingspan estimated sampled from a known distribution in comparison to distance estimated using an assumed 1 m wingspan, red line indicates where points would lie if there were a perfect match between the two. (Right) Distribution of root mean squared error (RMSE) of estimated

distance using a sampled wingspan estimate in comparison to an assumed 1 m wingspan, red line indicates median RMSE of 76 m.

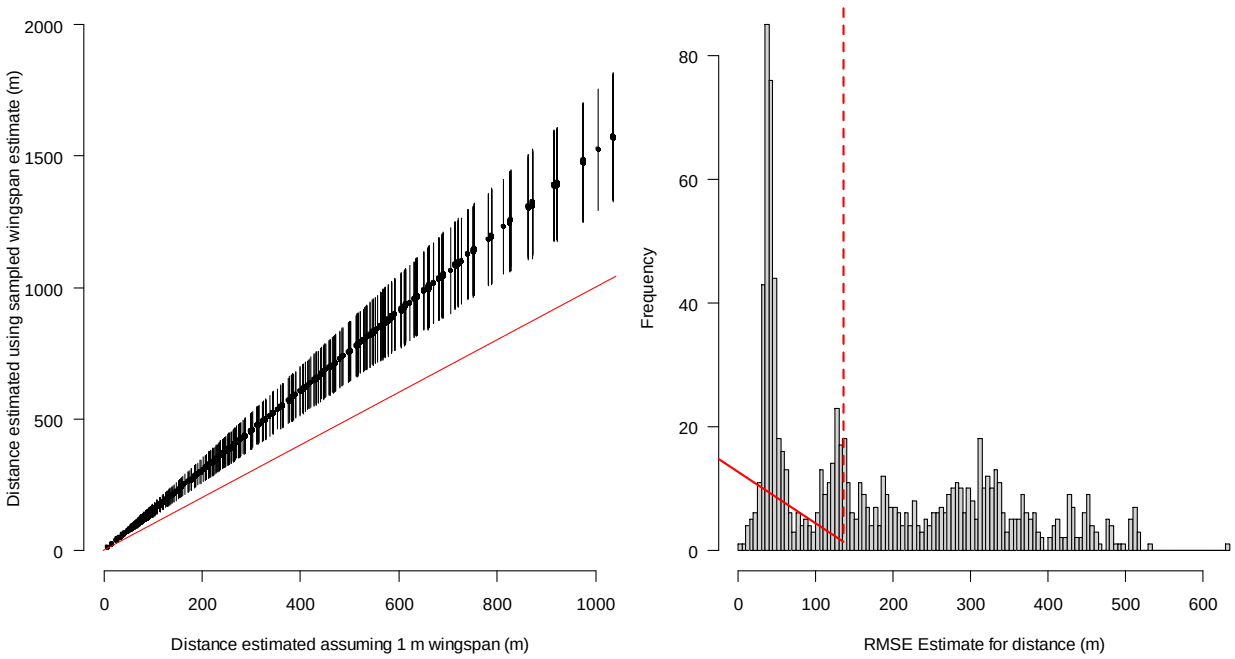

Figure R15. (Left) Distance estimated for unidentified gulls using a wingspan estimated sampled from a known distribution in comparison to distance estimated using an assumed 1 m wingspan, red line indicates where points would lie if there were a perfect match between the two. (Right) Distribution of root mean squared error (RMSE) of estimated distance using a sampled wingspan estimate in comparison to an assumed 1 m wingspan, red line indicates median RMSE of 137 m.

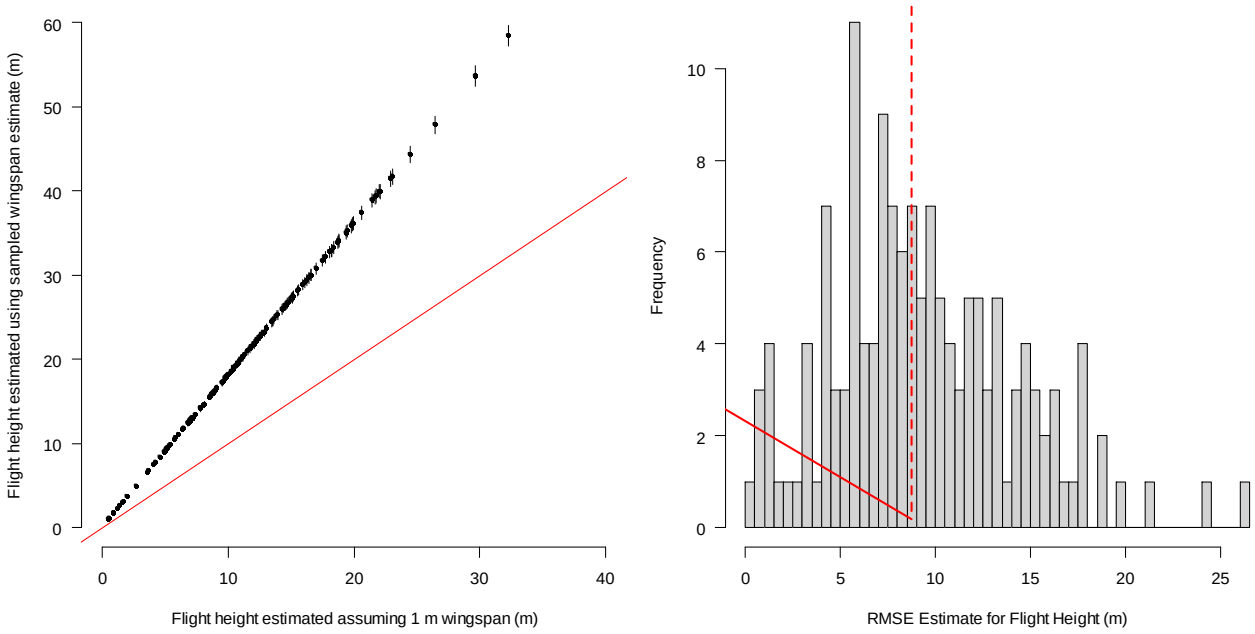

Figure R16. (Left) Flight height estimated for gannets using a wingspan estimated sampled from a known distribution in comparison to distance estimated using an assumed 1 m wingspan, red line indicates where points would lie if there were a perfect match between the two. (Right) Distribution of root mean squared error (RMSE) of estimated flight height using a sampled wingspan estimate in comparison to an assumed 1 m wingspan, red line indicates median RMSE of 8.76 m.

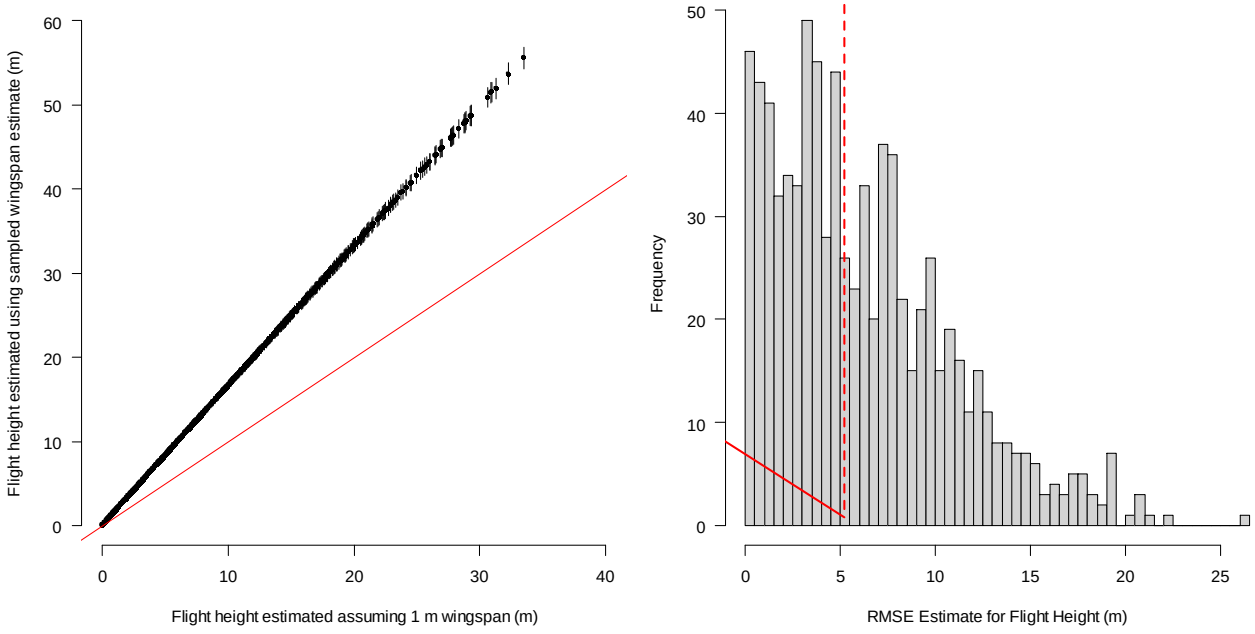

Figure R17. (Left) Flight height estimated for great black-backed gulls using a wingspan estimated sampled from a known distribution in comparison to distance estimated using an assumed 1 m wingspan, red line indicates where points would lie if there were a perfect match between the two. (Right) Distribution of root mean squared error (RMSE)

of estimated flight height using a sampled wingspan estimate in comparison to an assumed 1 m wingspan, red line indicates median RMSE of 5.19 m.

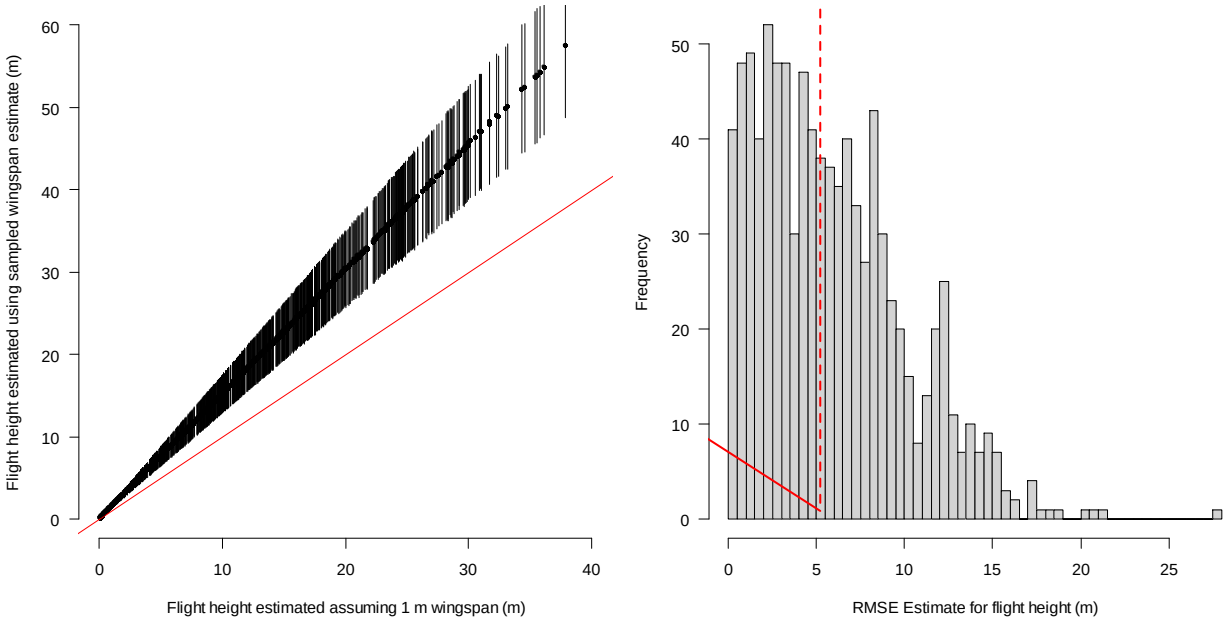

Figure R18. (Left) Flight height estimated for unidentified gulls using a wingspan estimated sampled from a known distribution in comparison to distance estimated using an assumed 1 m wingspan, red line indicates where points would lie if there were a perfect match between the two. (Right) Distribution of root mean squared error (RMSE) of estimated flight height using a sampled wingspan estimate in comparison to an assumed 1 m wingspan, red line indicates median RMSE of 5.21 m.

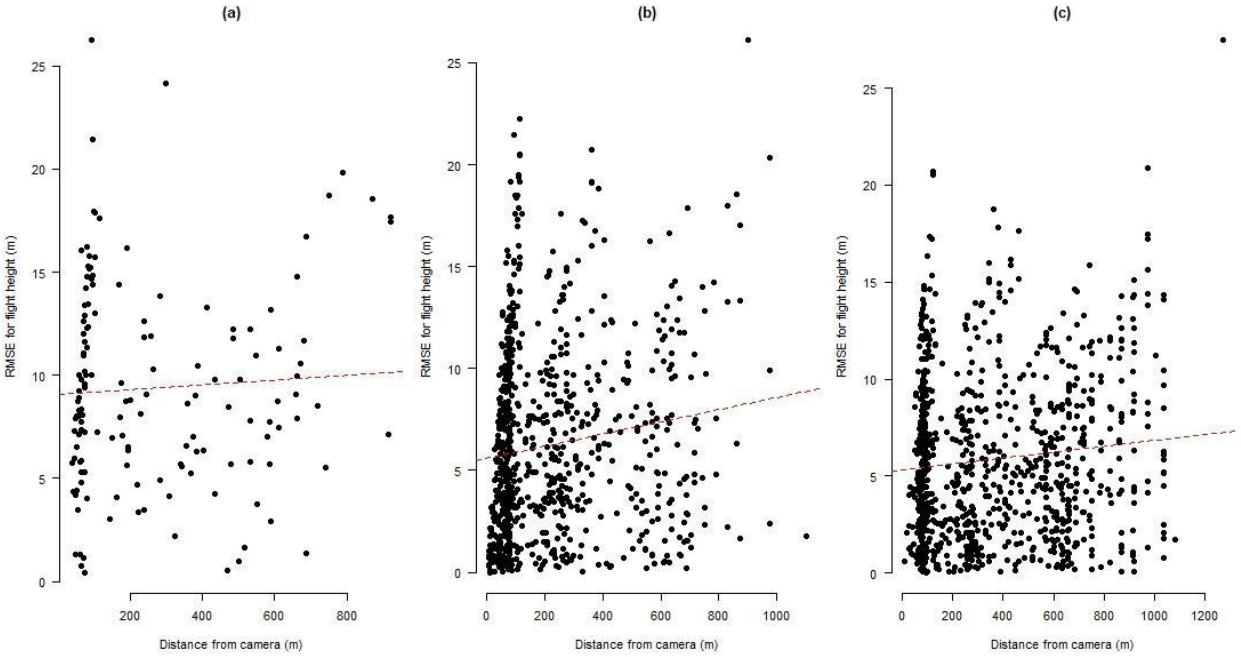

Figure R19. Relationship between root mean squared error (RMSE) estimates of flight height and distance from camera for (a) gannets; (b) great black-backed gulls; and, (c) unidentified gulls.

Flight Direction

Species

As might be expected given the dominance of great black-backed gull, and other gull species, in the dataset, the flight directions for all birds largely corresponded to the flight directions for gulls (Figure R20). Whilst flights were generally in a westerly direction, there was no clear dominant direction (mean flight direction for all observations 261° SD 34°), with the possible exception of gannets, which appeared to fly along an SE-NW axis (mean flight direction 179° SD 24°), indicated by more pronounced peaks in the NW and SE segments of the plot for Northern Gannet in Figure R20.

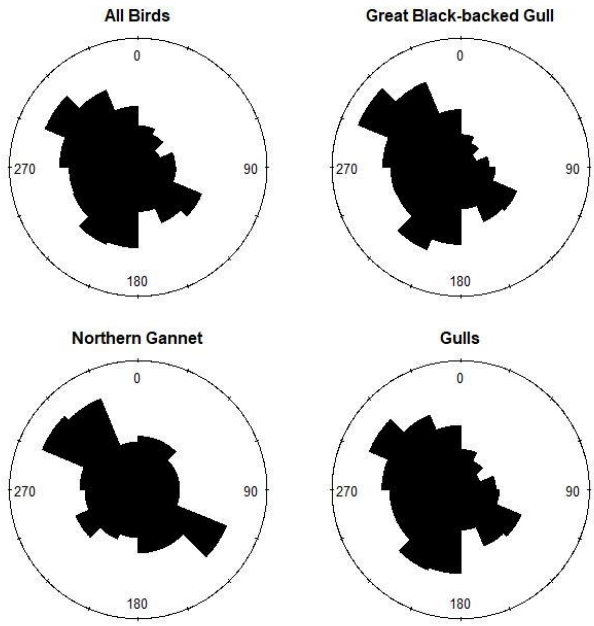

Figure R20. Flight directions for all birds detected, great black-backed gull, northern gannet and all gulls.

Camera

Flight directions for the Viewpoints A (mean 251° SD 41°) and B (mean 250° SD 34°), within the wind farm, were broadly similar, and consistent with the flight directions for all species highlighted above. However, flight directions at Viewpoint C (mean 280° SD 29°) showed more evidence of directional flight along an SE-NW axis (Figure R21).

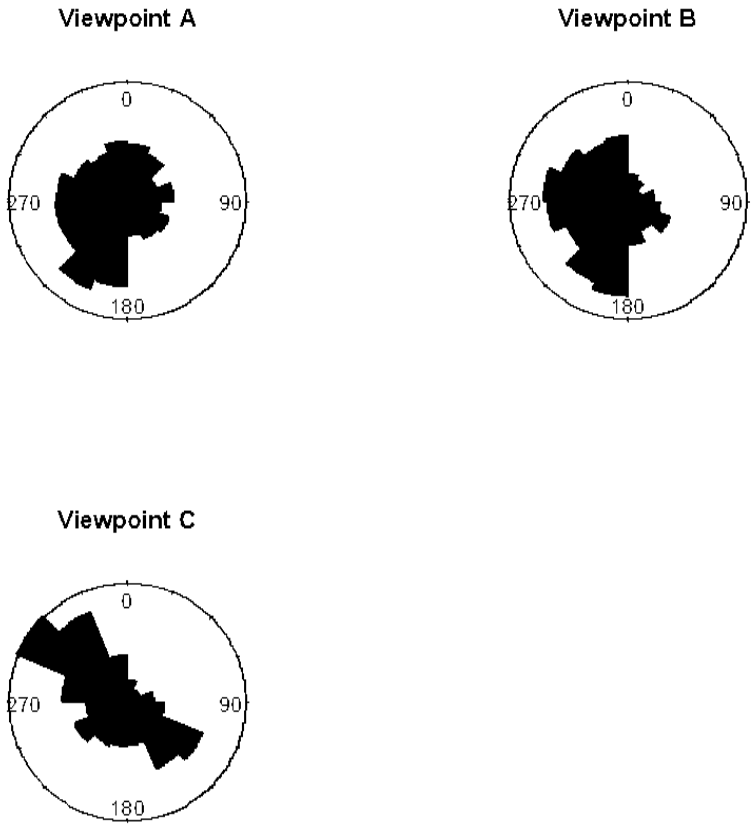

Figure R21. Flight directions for all birds detected from viewpoints A, B and C.

Year

There appeared to be a slight difference in the overall flight directions recorded in 2023 (mean 258° SD 37°) and 2024 (mean 280° SD 31°) (Figure R22), largely driven by differences in the directions recorded at Viewpoint A (Table R8).

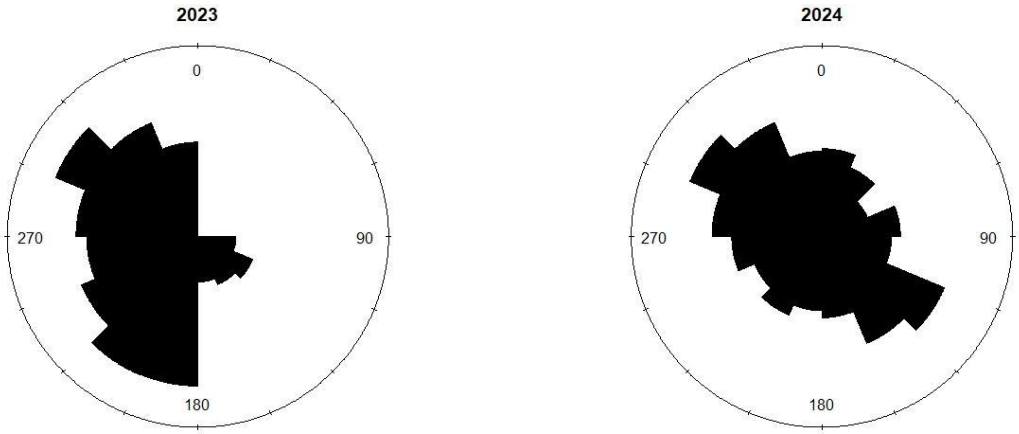

Figure 22. Flight directions for all birds detected in 2023 and 2024

Table R8. Mean flight directions by year for Viewpoints A, B and C.

	Viewpoint A	Viewpoint B	Viewpoint C
2023	236° (SD 45°)	`249° (SD 37°)	280° (SD 30°)
2024	300° (SD 37°)	255° (SD 28°)	268° (SD 27°)

Season

There were clear differences in the flight directions recorded in the spring (mean 164° SD 27°) and the summer (mean 267° SD 33°), autumn (mean 263° SD 37°) and winter (236° SD 40°). This difference was evident amongst the three main species groups (Table R9, Figure R23), and from Viewpoints A and C, but not Viewpoint B (Table R10).

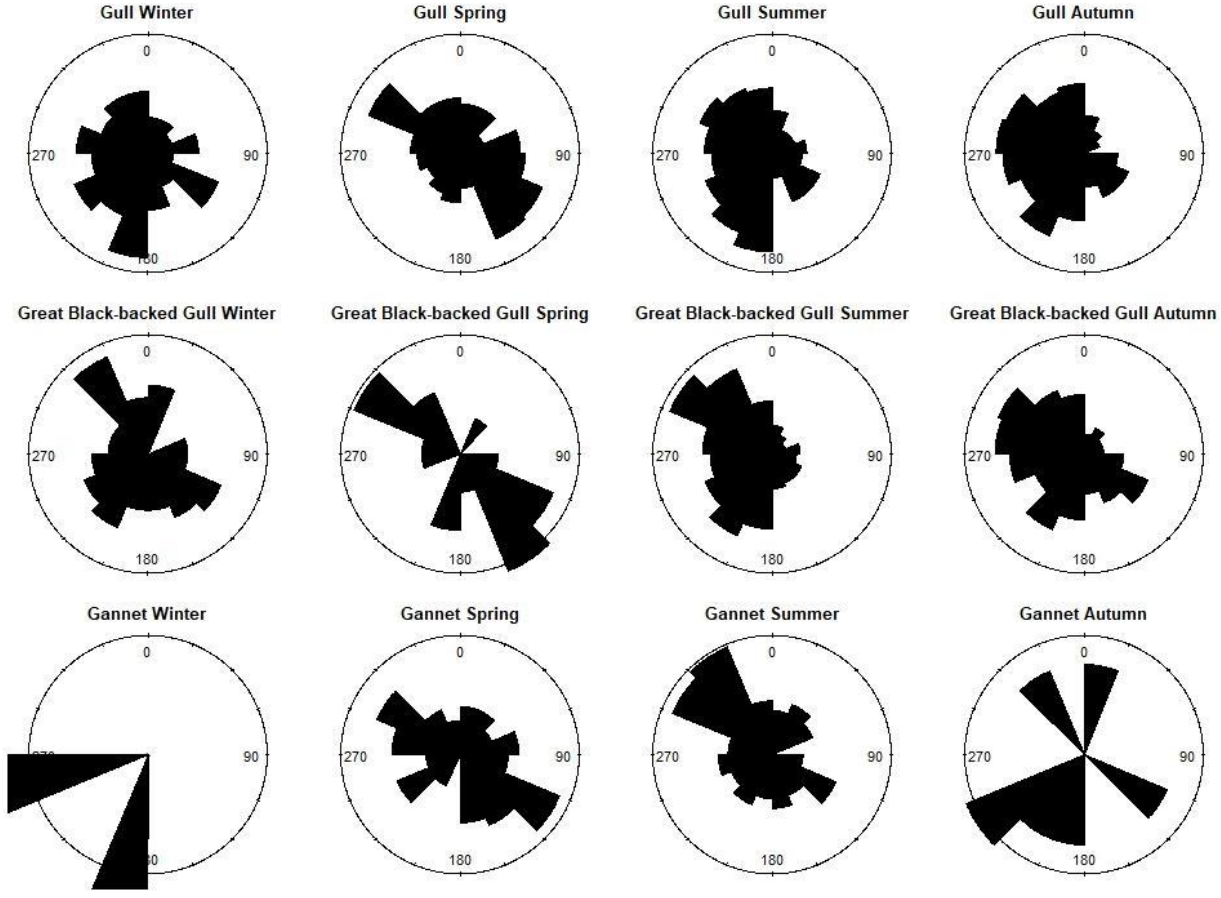

Figure R23. Flight directions for different species groups by season

Table R9. Mean flight directions by season for different species groups.

	Winter	Spring	Summer	Autumn
Gull	227° (SD 42°)	108° (SD 22°)	250° (SD 34°)	266° (SD 34°)
Great black-backed Gull	256° (SD 31°)	171° (SD 26°)	272° (SD 33°)	259° (SD 37°)
Gannet	220° (SD 16°)	158° (SD 34°)	302° (SD 27°)	225° (SD 70°)

Table R10. Mean flight directions by season for Viewpoints A, B and C.

	Winter		Spring		Summer		Autumn	
	2023	2024	2023	2024	2023	2024	2023	2024
Viewpoint A	250° SD 49°	164° SD 47°	-	68° SD 34°	236° SD 43°	309° SD 37°	233° SD 46°	292° SD 38°
Viewpoint B	261° SD 52°	169° SD 37°	-	268° SD 26°	246° SD 35°	148° SD 29°	251° SD 37°	278° SD 23°
Viewpoint C	268° SD 36°	112° SD 22°	295° SD 24°	164° SD 24°	287° SD 29°	319° SD 26°	257° SD 32°	308° SD 40°

Error

For the data collected at Hywind Tampen, the difference between these mean randomly sampled bearings, and those estimated based on the first and last point of each track is typically quite low, at an average of ~7.5°across all species, though in some cases it was more substantial (Figure R24). The standard deviation (mean SD 34°) in flight direction within each track was of a similar magnitude to the standard deviation in direction across all tracks, estimated above (Tables R7 – R9), arising as a result of factors such as differences between seasons, years and viewpoints. This suggests that the uncertainty introduced into estimates of flight direction through a simplified approach of comparing the first and last point on each track is of a similar magnitude to that introduced through background variability in the data.

Comparison of differences in the two approaches to estimating flight direction may help inform inferences of bird behaviour. Behaviours such as foraging would be characterised by tracks with a greater sinuosity than is the case for birds engaged in migratory or commuting flight (Amélineau *et al.* 2021). During migration, which is likely to be characterized by more directional flight, we would expect birds to be traveling in straight lines, meaning that there would be a smaller difference between flight directions estimated based on mean randomly sampled bearings, and those estimated based on the first and last point of each track, than would be the case for foraging flight. Similarly, we would expect a smaller standard deviation around directions estimated based on mean randomly sampled bearings for migratory than foraging flight.

During the spring, and at Viewpoint C, the difference between the mean randomly sampled bearings, and those estimated based on the first and last point of each track are lower than is the case for other times of year, or Viewpoints A and B (Tables R11 and R13). This is also the case for gannets in comparison to gulls. These data suggest that there may be a difference in behaviour between birds within the wind farm, recorded from Viewpoints A and B, and those on the edge of the wind farm, recorded from Viewpoint C.

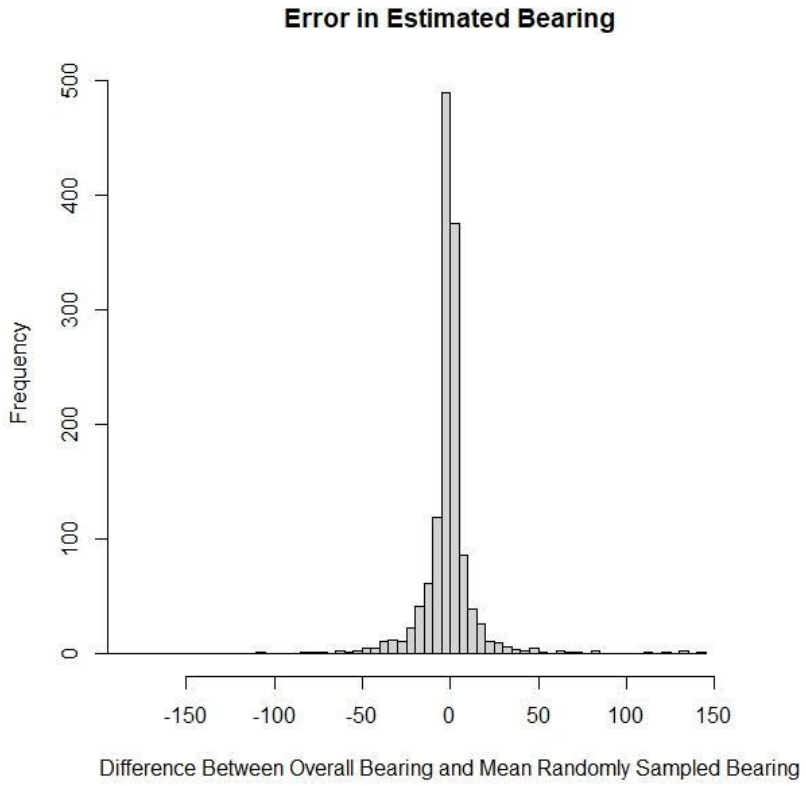

Figure R24. Distribution of differences between the overall bearing estimated based on the first and last point of each track and the mean bearing estimated between randomly sampled points

Table R11. Mean differences between the overall bearing estimated based on the first and last point of each track and the mean bearing estimated between randomly sampled points for each season and species

	Winter	Spring	Summer	Autumn
All Birds	9.24° (SD 14.97°)	4.40° (SD 6.75°)	7.61° (SD 14.89°)	8.28° (SD 12.51°)
Gulls	9.25° (SD 13.98°)	4.02° (SD 6.33°)	8.11° (SD 16.74°)	7.90° (SD 10.45°)
Gannet	2.51° (SD 0.01°)	5.27° (SD 7.29°)	4.91° (SD 6.39°)	8.47° (SD 7.51°)
Great black-backed Gull	6.08° (SD 9.85°)	2.73° (SD 3.64°)	8.16° (SD 16.74°)	8.86° (SD 14.49°)

Table R12. Mean differences between the overall bearing estimated based on the first and last point of each track and the mean bearing estimated between randomly sampled points for each viewpoint and species

	Viewpoint A	Viewpoint B	Viewpoint C
All Birds	9.22° (SD 11.86°)	8.34° (SD 16.80°)	5.61° (SD 11.80°)
Gulls	8.47° (SD 11.13°)	7.36° (SD 13.35°)	6.60° (SD 14.71°)
Gannet	6.73° (SD 7.17°)	8.44° (SD 9.45°)	3.55° (SD 5.12°)
Great black-backed Gull	10.35° (SD 12.61°)	9.79° (SD 21.26°)	5.54° (SD 10.73°)

Testing reduced file size

In figures R25 and R26, the results from analysing the 30 FPS videos from December 2023 and the 10 FPS videos from December 2024 are shown, respectively. Figure R25 shows that birds are detected and tracked by Spoor software, even at the lower framerate of 10 FPS. Although, the total bird detection counts were lower for December 2024 than the same month in 2023, this difference is similar to what we found in general for 2024 versus 2023 (Figure R10) and is therefore more likely due to natural variation than an effect of reducing frame rate during the December 2024 period. For reference, the total bird count for December 2024 was 90 compared to 154 for December 2023 and the average file size for a 5-minute video segment for the 30 FPS 2023 data was 165 Mb compared to 16 Mb for the 10 FPS 2024 data. Thus, a significant reduction in data storage appears possible without a large impact on the results obtained.

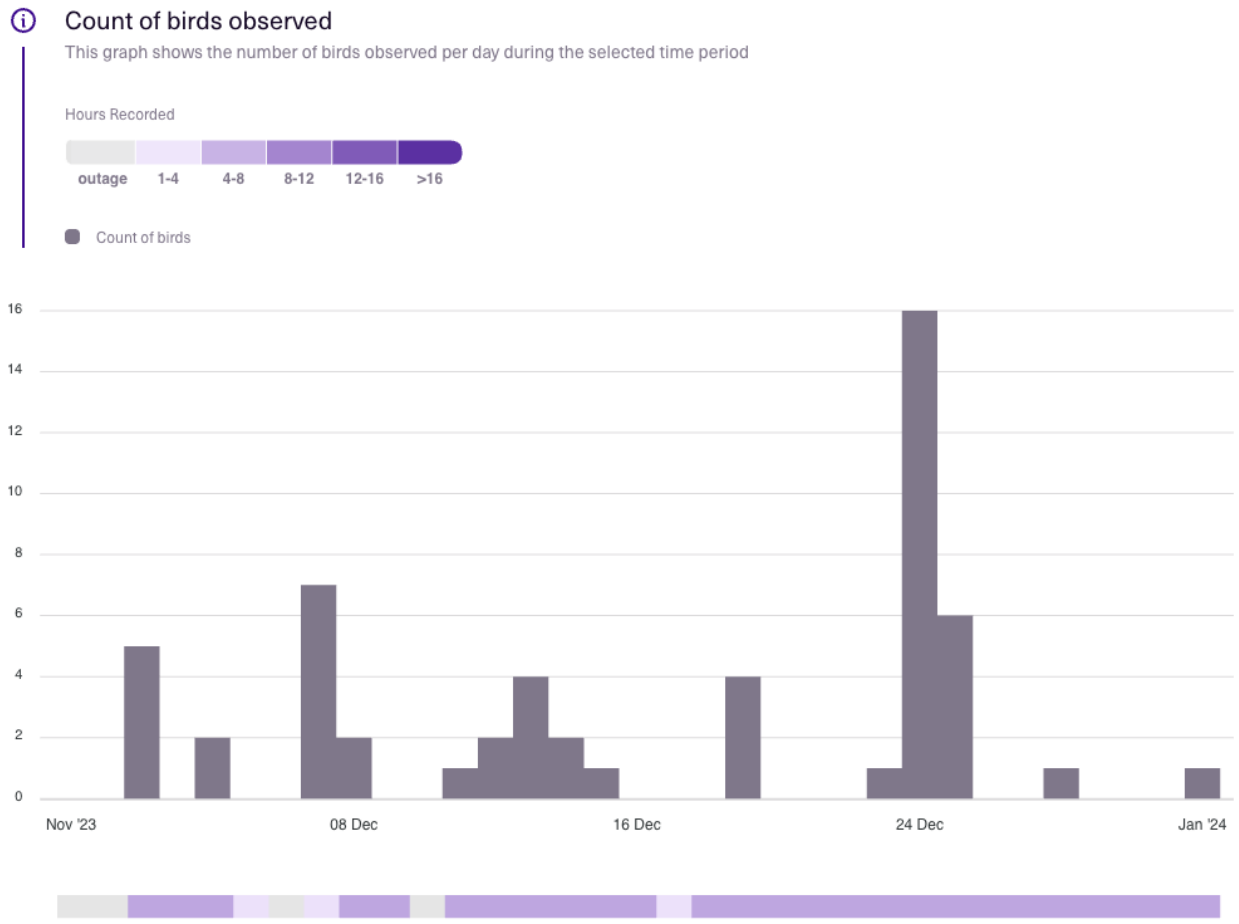

Figure R25. Bird observation counts from all three cameras for December 2023.

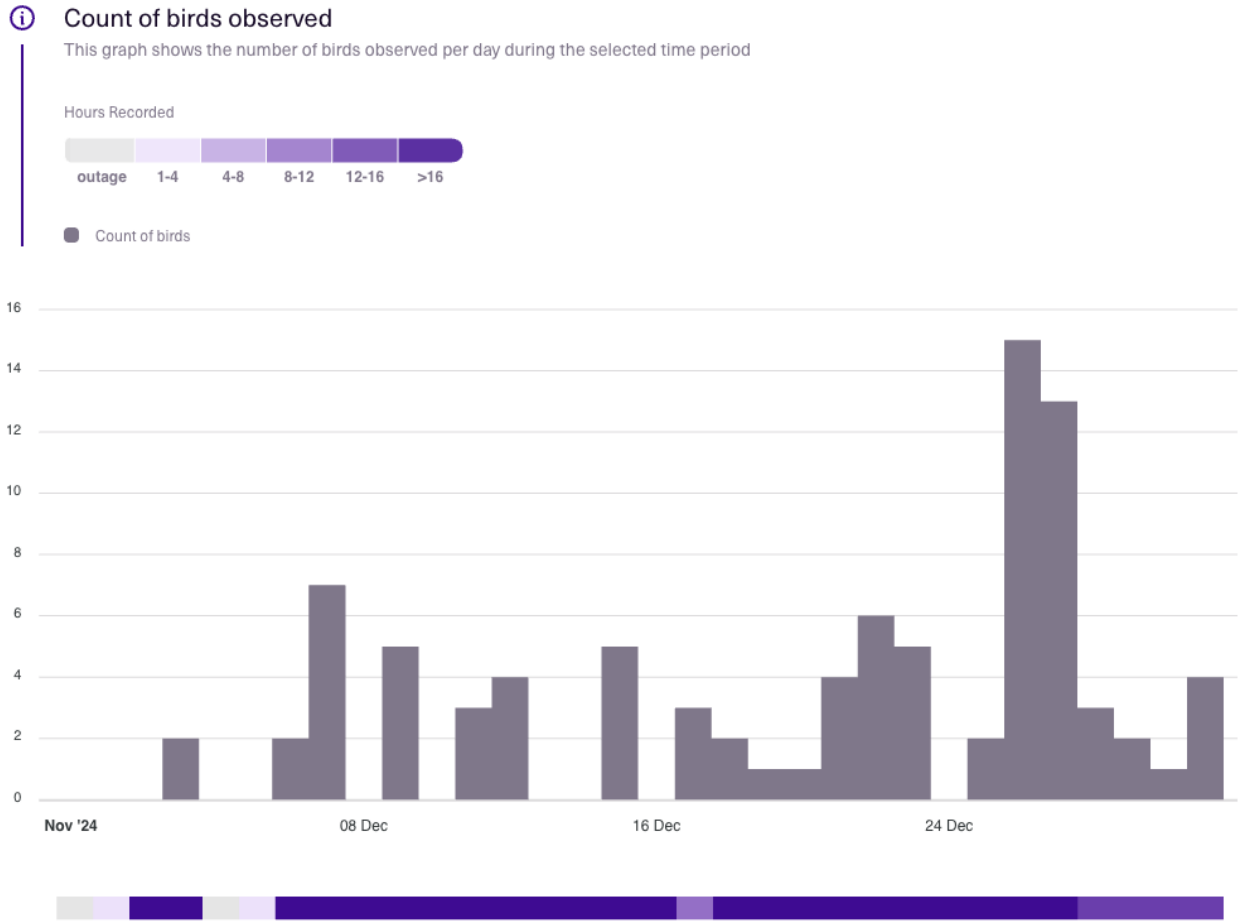

Figure R26. Bird observation counts from all three cameras for December 2024.

Discussion

System performance

Patterns of bird abundance at Hywind Tampen

Species identification, occurrence, detection distance and tracking duration

89% of all bird observations could be classified to species (46%), family (42%) or order (1%) level, leaving only 11% of all bird observations unidentified to taxonomic levels of class or lower. Of the detected species, the white wagtail is the smallest with a wingspan of 25-30 cm, and the Northern gannet is the largest with a wingspan of 165-185 cm.

The list of detected species indicates that it is mainly breeding and/or wintering seabirds that were captured by Spoor AI. The exceptions were small passerines, barn swallows, a woodpecker, an owl, and raptors, which were largely restricted to the spring or autumn migration periods, and hence likely to reflect migrating birds (with the exception of the woodpecker, which is likely to reflect the movement of a juvenile or immature bird).

Whilst the migration period does not seem to significantly affect the detection counts at Hywind Tampen, records of barn swallows and a short-eared owl during spring are likely to reflect migrating birds. Looking at the seasonal distribution of species observations in Table R1, even though the most diverse bird occurrences were during the summer and autumn, the taxa observed exclusively during those periods had low counts (~<10) (e.g., Northern fulmar, raptors).

The analysis of the minimum and maximum bird detection distances provided valuable insights into the camera system's capabilities. The findings were most meaningful for species with a higher number of detections, such as the Great Black-backed Gull. Generally, detection patterns were consistent across species and indicated that most birds are first observed within approximately 100 meters of the cameras, rather than at greater distances. A small number of group-level taxonomic observations (e.g., gulls; birds) were made into the thousands of meters.

The above have important ramifications in the choice of cameras to use depending on the purpose of the survey. Viewpoint C, which had the greatest detection space within the first hundreds of meters, and was most useful for recording bird ID (~53% of birds identified to species level) and abundance in the vicinity of the wind farm. In contrast, Viewpoint A was best at observing birds far away but relatively poor at assigning IDs to them (~37% of birds identified to species level), and with a field of view that meant less coverage of areas closer to the wind farm, hence, it could be useful if bird numbers only were of importance. Viewpoint B with intermediate capabilities may represent an effective compromise between detection space and species identification. Finally, it

is worth noting, that after data normalisation has been applied to account for the different viewpoint detection capabilities, the reduced dataset is still dominated by Viewpoint C, indicating a greater abundance of birds outside, than inside the wind farm. Ultimately, the best normalisation method is conducted pre-survey by using similar camera settings across all viewpoints, rather than post-survey. While the latter is still possible, as evidenced in this study, it still has limitations that need to be considered when interpreting the results.

Temporal variability

The highest absolute number of observations was 931 and occurred during the summer, followed by 684 observations during the autumn, 306 in winter, and 271 in spring (Table R1). However, this does not account for recording duration, which was almost double during summer and autumn, in part reflecting seasonal changes in day length. Consequently, following the initial step to produce the normalised dataset, accounting for these temporal differences, no seasonal effect in daily observed abundances was detected (Figure R9). The seasonal patterns only became apparent in the reduced dataset with an equalised detection space across all three cameras (Table R4; Figure R9). Within the reduced dataset, abundance peaked during the late summer and early autumn, likely to correspond to the point at which gull species, which dominate the birds detected during this study, depart breeding colonies and begin their migration (e.g. Borrmann *et al.* 2021). Further evidence for the possible influence of migration is available when considering the observed flight directions in the full dataset which highlighted clear differences in flight direction between the spring (mean 164° SD 27°) and the rest of the year. This difference was evident amongst the three main species groups, and from Viewpoints A and C. It is likely to reflect spring migration with species, including gulls and gannets, returning to their breeding sites from their wintering locations. The smaller standard deviation around the mean values from spring may also reflect more directional flight, as might be expected during migration.

Focusing on interannual variations, 2023 had overall significantly higher abundances compared to 2024. Seabird distributions at sea are often closely linked to oceanographic features, such as the location of fronts, which may vary over time (Robertson *et al.* 2014; Warwick-Evans *et al.* 2016). Consequently, interannual variation in distributions are a common feature of seabird at sea data, but without more detailed environmental data, it is not possible to investigate the reasons for these patterns.

Impact of environmental conditions

Foggy conditions significantly reduced detection distances but not tracking duration. Additionally, there was no difference between the rest of the weather conditions (cloudy, rainy, clear) in terms of bird detection distances and weather conditions. It must be noted that environmental data used in this survey were taken from 140 km away, hence, might not represent local conditions at Hywind Tampen.

Modelling results identified confirmed the significant effect of survey year and survey month as important drivers of daily bird abundances at Hywind Tampen (Tables R3 and R4). Wind speed was also identified as being negatively correlated with abundance when using the full dataset. As

mentioned above, local environmental data will provide more certainty in the above results. Notably, local environmental data might lead to the opposite effect, in that conditions not identified as significant here (temperature, wind direction, weather conditions) might become significant, in line with existing literature (Garthe *et al*. 2009; Gibb *et al*. 2017; Pistorius *et al*. 2015).

Comparing the models based on the reduced and normalized dataset, respectively, even though the former has slightly better capabilities of predicting abundance patterns (higher deviance and lower GCV values; Table R4), the difference with the normalized dataset model is minor. Given that the normalized-dataset model has a higher explanatory power (higher adjusted R^2 values, Table R3), and because it provides more insight into the role of wind speed, it is more useful for understanding ecological drivers of bird populations.

Finally, one unquantified effect on the above daily abundance rates could be due to water droplets on the lens/es that might have suppressed counts during rainy conditions

Error, bias, precision, variability and uncertainty

The potential for uncertainty in data collected in relation to offshore wind farms has been widely acknowledged (e.g. Masden *et al.* 2015; Searle *et al.* 2023). This uncertainty can arise as a consequence of natural variability in the environment and/or as a result of differences in error, bias and precision introduced during data collection. It is important to acknowledge that this is a common feature of all biological data collection, regardless of the methodology or technology used (Elphick 2008). However, in order to ensure that robust inferences can be made in relation to the data collected as part of ecological studies, it is vital to clearly define, identify and, where possible, quantify, error, bias and precision, and the contribution that these make to any uncertainty in the available data. We discuss these in turn below.

Error

Measurement error is a common feature of movement data (Jerde & Visscher 2005). Figures R13-R18 highlight how assumptions around species wingspan introduce error into estimates of the distance between the camera and the bird, and of the flight height of the bird. It is important to understand, and where possible, quantify this error.

Error may be systematic and/or random, and it is important to understand the extent of each. Over-, or underestimating species wingspans introduces a systematic error into estimates of the distance between the camera and the bird concerned (Figures R13-R18), resulting in a consistent over- or underestimate of both distance and flight height, depending on the species concerned. Of particular note is that this error appears correlated with distance, meaning that the impact of inaccuracies in assessments of species wingspan is greater at increased distances from the camera. Systematic errors such as this will introduce bias into the final estimated locations of the birds.

There is intra-specific variation in species body sizes. As a consequence, it is not possible to have a high degree of certainty surrounding the real world size of the bird used in Eq. 3. This uncertainty will introduce error into estimates of the location of the birds (Boersch-Supan *et al.* 2024). However, this error is likely to be random, rather than systematic, meaning that it will influence the precision of any estimates, but is unlikely to introduce any additional bias.

Bias

Bias in the data may arise either due to systematic errors, or due to study design. Systematic errors introduced bias through over- or underestimating values. For example, where species wingspans are greater than 1 m, the assumption of a 1 m wingspan results introduces bias into the estimate of the distance between the camera and the bird by underestimating the true value (Figures R13 – R18).

Study design can introduce bias into data collection if certain areas are over or under-represented in sampling. For example, the field of view of the cameras used for data collection means that sampling volume increases with distance (Figure R1). As a consequence, birds closer to the camera are less likely to be within the field of view, and are therefore likely to be under-represented in the final dataset, than birds that are further away. Similarly, the height and pitch of the cameras will introduce bias into estimates of species flight heights as the resulting field of view does not cover the sea surface and lower altitudes, where many species are likely to be most abundant (Johnston et al. 2014). In the case of the cameras installed within Hywind Tampen, the tilt and pitch means that the minimum height above sea-level covered is ~19 m (Figure R1). Consequently, birds below this height will not be detected, which for many species is likely to constitute the majority of those present (Johnston *et al.* 2014). As a result, estimated mean flight heights and distributions for the species detected will be biased, and over-estimated in relation to the ”true” values (Table R6, Figure R11).

In some instances, these sampling biases can be accounted for by correcting for area sampled. However, such corrections assume either that birds are randomly distributed with respect to the position of the camera, or that any non-randomness can be easily accounted for. Birds are known to be non-randomly distributed in relation to both height above sea-level (Johnston *et al.* 2014), and with distance to turbines (Johnston *et al.* 2022; Pollock *et al.* 2024). Accounting for both of these processes, particularly whilst there is still substantial uncertainty associated with them, is extremely challenging.

Without accounting for biases in the data collected, comparisons of the numbers of birds present at different locations and time periods must be limited to relative, rather than absolute numbers. Furthermore, differences in the field of view and sampling volume of the cameras used in this study, mean that these comparisons must be made using a normalised estimate of birds within a common detection space.

Precision

Precision relates to the extent of any error associated with the estimated location. As highlighted in figures R13-R18, there can be a high degree of precision associated with these estimates – as indicated by the relatively tight standard deviations around the locations estimated by randomly sampling wingspans from distributions of known values – but these estimates may still be subject to substantial error – as indicted the estimates of RMSE between locations estimated based on an assumed 1 m wingspan, and wingspans estimated from distributions of known values. Typically, the precision with which we are able to estimate values will increase as we obtain better information and data. For example, where we are able to estimate the distance between then camera and great black-backed gulls with greater precision (Figure R14) than is the case for unidentified gulls (Figure R15). However, care must be taken to ensure that any estimates are not unduly precise. For example, in addition to considering uncertainty in species wingspan, calculations may need to account for the potential for the angle of the bird relative to the camera to influence the real-world width of the bounding box considered in Eq. 3. Failing to do so may give a misleading impression of the uncertainty associated with estimated positions.

Variability

The numbers and species of birds recorded, and their flight behaviours will be influenced by spatial, temporal and environmental variability. Analyses highlighted that abundance was greater in 2023 than in 2024, and that there were seasonal patterns in the number of birds recorded (Figure R9). Similarly, considering the data on flight directions, there were clear differences between Viewpoint C, outside the wind farm, and Viewpoints A and B, inside the wind farm. By quantifying, and accounting for, these relationships, for example by applying analyses such as those presented above (Tables R3 and R4), it is possible to reduce some of the uncertainty associated with the numbers of birds seen, and their behaviour.

Uncertainty

Uncertainty is a common feature of ecological data (Milner-Gulland & Shea 2017). It arises as a function of error, bias, precision and variability associated with the data under consideration. Reducing the uncertainty associated with the CCTV data will increase the value of these data for understanding species interactions with offshore windfarms. However, it is important to acknowledge that that, as with all ecological data, there will be an element of irreducible uncertainty. Consequently, it is important to consider which elements of uncertainty can be reduced, and which cannot. For example, errors in estimates of the position of birds introduced through assumptions of a standard 1 m wingspan can be reduced through the use of readily species-specific estimates, where birds can be identified to species, or group, level. However, natural variation in species body size means that there will be limit to the precision that can be achieved using this approach (Boersch-Supan *et al.* 2024). Consequently, uncertainty can be reduced by reducing the error introduced through assumptions about species body size, but not through improvements in the precision of these estimates.

Reduced file size

Although it was necessary to use data from different periods for the analysis and comparing 30 FPS and 10 FPS videos (and therefore the experiment was not controlled), the conclusion is that the system is still able to detect and tracks birds at 10 FPS and visually the results look similar to results obtained when analysing 30 FPS videos. There likely is some reduction in the ability to detect and track birds with 10 FPS versus 30 FPS videos, however do not appear significant. Therefore, given that the frame rate reduction yields more than an order of magnitude reduction in file size, Spoor does not see any problem reducing the frame rate to 10 FPS for the purpose of bird monitoring from CCTV cameras and Hywind Tampen going forward.

Conclusions and recommendations

The CCTV cameras at Hywind Tampen collect valuable data describing the movements of birds in and around the wind farm. As might be expected, the species detected are dominated by seabirds with substantial foraging ranges (Woodward *et al.* 2024). However, there was a clear signal in relation to migration both in relation to the species detected, and the flight directions recorded, particularly during the spring. Camera data also indicated potential differences in flight direction inside and outside the wind farm, and evidence of more directional flight outside the wind farm, indicative of possible differences in behaviour. It would be valuable to explore these relationships in more detail to gain a greater understanding of species responses to offshore wind farms, potentially through comparison with data collected using the buoy-mounted cameras deployed at the site. By including environmental data from closer to the wind farm in analyses, it would be possible to more clearly quantify drivers of changes in daily bird abundance, particularly in relation to weather conditions.

The analyses presented here highlight that, whilst post-survey normalisation methods are possible, they can have limitations (e.g. favouring the camera on which the thresholds for the equal detection space have been based on; in this case Viewpoint C) and remove a significant part of the collected data in the process. These limitations can be overcome during the study design phase through the selection of cameras with similar, and ideally identical, detection capabilities, which would make for a more straightforward comparison of data. Normalisation was based on birds/sampling volume/unit time, a commonly used approach that can provide standardised information on species abundances. These data could potentially be scaled up to the level of the wind farm, which may provide a useful measure of flux as an input to collision risk models (Cook *et al.* 2025). Through comparison with data collected during pre-construction surveys, for example using buoy-mounted cameras, data may also be used to make inferences about changes in abundance and displacement rates. Further development of normalisation methods, for example consideration of total bird minutes recorded, rather than bird abundance, may yield further insights into bird behaviour that complement other findings.

A key source of uncertainty in location of the tracks obtained from the data arises from errors introduced by an assumption of a generic 1 m wingspan for all species. Errors in estimated flight

heights are of a magnitude similar to those obtained using GPS tagging (Johnston *et al.* 2023), and substantially smaller than those obtained using digital aerial survey (Boersch-Supan *et al.* 2024). However, error in the estimates of horizontal distance between the camera and bird are more substantial, which may be of significance if estimating the proximity of birds to turbines. Where birds have been identified to species, or group level, this error could be reduced through the use of published estimates of wingspan (e.g. Snow & Perrins 1998). However, there is likely to be a limit to the precision that can be achieved using this approach as a consequence of natural variation in species body size.

References

Amélineau, F., Merkel, B., Tarroux, A., Descamps, S., Anker-Nilssen, T., Bjørnstad, O., Bråthen, V.S., Chastel, O., Christensen-Dalsgaard, S., Danielsen, J., Daunt, F., Dehnhard, N., Ekker, M., Erikstad, K.E., Ezhov, A., Fauchald, P., Gavrilo, M., Hallgrimsson, G.T., Hansen, E.S., Harris, M.P., Helberg, M., Helgason, H.H., Johansen, M.K., Jónsson, J.E., Kolbeinsson, Y., Krasnov, Y., Langset, M., Lorentsen, S.H., Lorentzen, E., Melnikov, M.V., Moe, B., Newell, M.A., Olsen, B., Reiertsen, T., Systad, G.H., Thompson, P., Thórarinsson, T.L., Tolmacheva, E., Wanless, S., Wojczulanis-Jakubas, K., Åström, J. & Strøm, H. (2021) Six pelagic seabird species of the North Atlantic engage in a fly-and-forage strategy during their migratory movements. *Marine Ecology Progress Series* 676: 127–144.

Artsdatabanken: Norsk rødliste for arter 2021 (2021). Available at: https://artsdatabanken.no/lister/rodlisteforarter/2021 (Accessed: 28 March 2024)

Boersch-Supan, P.H., Brighton, C.H., Thaxter, C.B. & Cook, A.S.C.P. (2024) Natural body size variation in seabirds provides a fundamental challenge for flight height determination by single-camera photogrammetry: a comment on Humphries et al. (2023). *Marine Biology* 171: 122.

Cook, A.S.C.P., Salkanovic, E., Masden, E., Lee, H.E. & Kiilerich, A.H. (2025) A critical appraisal of 40 years of avian collision risk modelling: How have we got here and where do we go next? *Environmental Impact Assessment Review* 110: 107717.

Elphick, C.S. (2008) How you count counts: the importance of methods research in applied ecology. *Journal of Applied Ecology* 45: 1313–1320.

Equinor: Hywind Tampen (n.d). Available at: https://www.equinor.com/energy/hywind-tampen (Accessed: 28 March 2024)

Evidently AI: Accuracy vs. precision vs. recall in machine learning: what's the difference? (n.d). Available at: https://www.evidentlyai.com/classification-metrics/accuracy-precision-recall (Accessed: 28 March 2024)

Garthe, S., Markones, N., Hüppop, O. and Adler, S., 2009. Effects of hydrographic and meteorological factors on seasonal seabird abundance in the southern North Sea. Marine Ecology Progress Series, 391, pp.243-255.

Gibb, R., Shoji, A., Fayet, A.L., Perrins, C.M., Guilford, T. and Freeman, R., 2017. Remotely sensed wind speed predicts soaring behaviour in a wide-ranging pelagic seabird. Journal of the Royal Society Interface, 14(132), p.20170262.

Global Biodiversity Information Facility: What is Darwin Core, and Why does it matter? (n.d.). Available at: https://www.gbif.org/darwin-core (Accessed: 5 April 2024)

Hernis (n.d.). PT9W HD IP. Retreived from https://www.hernis.com/docs/dynamic/DSHE097164%20C%20PT9W%20HD%20IP.pdf

Jerde, C.L. & Visscher, D.R. (2005) Gps Measurement Error Influences on Movement Model Parameterization. *Ecological Applications* 15: 806–810.

Johnston, A. & Cook, A.S.C.P. (2016) How high do birds fly? Development of methods and analysis of digital aerial data of seabird flight heights. BTO Research Report No. 676. British Trust for Ornithology, Thetford. https://www.bto.org/research-data-services/publications/research-reports/2016/how-high-do-birds-fly-development-methods

Johnston, A., Cook, A.S.C.P., Wright, L.J., Humphreys, E.M. & Burton, N.H.K. (2014) Modelling flight heights of marine birds to more accurately assess collision risk with offshore wind turbines. *Journal of Applied Ecology* 51: 31–41.

Johnston, D., Thaxter, C., Boersch-Supan, P., Humphreys, E., Bouten, W., Clewley, G., Scragg, E., Masden, E., Barber, L., Conway, G., Clark, N., Burton, N. & Cook, A.S.C.P. (2022) Investigating avoidance and attraction responses in lesser black-backed gulls Larus fuscus to offshore wind farms. *Marine Ecology Progress Series* 686: 187–200.

Johnston, D.T., Thaxter, C.B., Boersch-Supan, P.H., Davies, J.G., Clewley, G.D., Green, R.M.W., Shamoun-Baranes, J., Cook, A.S.C.P., Burton, N.H.K. & Humphreys, E.M. (2023) Flight heights obtained from GPS versus altimeters influence estimates of collision risk with offshore wind turbines in Lesser Black-backed Gulls Larus fuscus. *Movement Ecology* 11: 66.

Masden, E.A., McCluskie, A., Owen, E. & Langston, R.H.W. (2015) Renewable energy developments in an uncertain world: The case of offshore wind and birds in the UK. *Marine Policy* 51: 169–172.

Milner-Gulland, E.J. & Shea, K. (2017) Embracing uncertainty in applied ecology. *Journal of Applied Ecology*.

The Norwegian Centre for Climate Services: Observations and weather statistics (n.d.). Available at: https://seklima.met.no/minutes/wind_from_direction/custom_period/SN76923/en/2023-05-01T00:00:00+02:00;2024-03-28T14:21:59+01:00 (accessed 28 March 2024)

Phillips et al. (2019). “Does perspective matter? A case study comparing Eulerian and Lagrangian estimates of common murre (Uria aalge) distributions. Ecology and Evolution, 9 (8), p.p. 4805-4819. https://doi.org/10.5061/dryad.1hg2n56.

Pistorius, P.A., Hindell, M.A., Tremblay, Y. and Rishworth, G.M., 2015. Weathering a dynamic seascape: influences of wind and rain on a seabird’s year-round activity budgets. PLoS One, 10(11), p.e0142623.

Pollock, C.J., Johnston, D.T., Boersch-Supan, P.H., Thaxter, C.B., Humphreys, E.M., O’Hanlon, N.J., Clewley, G.D., Weston, E.D., Shamoun-Baranes, J. & Cook, A.S.C.P. (2024) Avoidance and attraction responses of kittiwakes to three offshore wind farms in the North Sea. *Marine Biology* 171: 217.

The Royal Society for the Protection of Birds: Great Black-backed Gull (n.d.). Available at: https://www.rspb.org.uk/birds-and-wildlife/great-black-backed-gull (Accessed 28 March 2024)

Searle, K.R., O’Brien, S.H., Jones, E.L., Cook, A.S.C.P., Trinder, M.N., McGregor, R.M., Donovan, C., McCluskie, A., Daunt, F. & Butler, A. (2023) A framework for improving treatment of uncertainty in offshore wind assessments for protected marine birds. *Journal of Marine Science* 13.

Snow, D.W. & Perrins, C.M. (1998) *The Birds of the Western Palearctic. Concise Edition. Volume 1. Non-passerines.* Oxford University Press, Oxford.

Waggitt, J.J., Evans, P.G.H., Andrade, J., Banks, A.N., Boisseau, O., Bolton, M., Bradbury, G., Brereton, T., Camphuysen, C.J., Durinck, J., Felce, T., Fijn, R.C., Garcia-Baron, I., Garthe, S., Geelhoed, S.C.V., Gilles, A., Goodall, M., Haelters, J., Hamilton, S., Hartny-Mills, L., Hodgins, N., James, K., Jessopp, M., Kavanagh, A.S., Leopold, M., Lohrengel, K., Louzao, M., Markones, N., Martinez-Cediera, J., O’Cadhla, O., Perry, S.L., Pierce, G.J., Ridoux, V., Robinson, K.P., Santos, M.B., Saavedra, C., Skov, H., Stienen, E.W.M., Sveegaard, S., Thompson, P., Vanermen, N., Wall, D., Webb, A., Wilson, J., Wanless, S. & Hiddink, J.G. (2019) Distribution maps of cetacean and seabird populations in the North-East Atlantic. Journal of Applied Ecology 1365-2664.13525.

Woodward, I.D., Thaxter, C.B., Owen, E., Bolton, M., Ward, R.M. & Cook, A.S.C.P. (2024) The value of seabird foraging ranges as a tool to investigate potential interactions with offshore wind farms. *Ocean & Coastal Management* 254: 107192.

Zhang et al. (2014). An Implementation of Document Image Reconstruction System on a Smart Device Using a 1D Histogram Calibration Algorithm. Mathematical Problems in Engineering. 2014. 1-10. 10.1155/2014/313452.

Appendix

Appendix Table 1: Summary of species observed and their threat status per survey year and viewpoint across both full and reduced dataset.

Common Name	Taxon	Norwegian Red List	Year	Obs	Viewpoint	Obs - Reduced
Barn swallow	*Hirundo rustica*	LC	2023	0	A	0
				0	B	0
				4	C	3
			2024	0	A	0
				0	B	0
				0	C	0
Bird	Aves		2023	48	A	4
				29	B	8
				47	C	11
			2024	44	A	3
				24	B	5
				55	C	27
Black-legged kittiwake	*Rissa tridactyla*	EN	2023	0	A	0
				3	B	3
				0	C	0
			2024	0	A	0
				0	B	0
				1	C	1
European herring gull	*Larus argentatus*	VU	2023	0	A	0
				0	B	0
				0	C	0
			2024	5	A	1
				0	B	0
				2	C	2
European Shag / Great Cormorant	*Phalacrocorax aristotelis / Phalacrocorax carbo*	LC* / NT	2023	0	A	0
				0	B	0
				0	C	0
			2024	0	A	0
				5	B	4
				0	C	0
Great black-backed gull	*Larus marinus*	LC	2023	141	A	22
				208	B	98
				278	C	163
			2024	63	A	13
				30	B	6
				96	C	73
Great skua	*Stercorarius skua*	LC*	2023	0	A	0
				0	B	0
				1	C	1
			2024	0	A	0

				0	B	0
				0	C	0
Great spotted woodpecker	*Dendrocopos major*	LC	2023	0	A	0
				0	B	0
				1	C	1
			2024	0	A	0
				0	B	0
				0	C	0
Gull	Laridae		2023	178	A	5
				157	B	19
				154	C	35
			2024	201	A	7
				71	B	6
				157	C	62
Northern fulmar	*Fulmarus glacialis*	LC	2023	8	A	0
				8	B	6
				1	C	0
			2024	0	A	0
				0	B	0
				0	C	0
Northern gannet	*Morus bassanus*	LC	2023	4	A	1
				8	B	3
				16	C	10
			2024	47	A	1
				18	B	6
				54	C	47
Raptor	Telluraves?		2023	0	A	0
				0	B	0
				1	C	1
			2024	1	A	0
				0	B	0
				0	C	0
Short-eared owl	*Asio flammeus*	LC*	2023	0	A	0
				0	B	0
				0	C	0
			2024	0	A	0
				0	B	0
				1	C	0
Small passerine bird	Passeriformes		2023	8	A	1
				2	B	0
				3	C	0
			2024	6	A	0
				0	B	0

				5	C	3
Wader	Charadriiformes		2023	2	A	0
				0	B	0
				0	C	0
			2024	0	A	0
				0	B	0
				0	C	0
White wagtail	*Motacilla alba*	LC	2023	0	A	0
				0	B	0
				1	C	1
			2024	0	A	0
				0	B	0
				0	C	0
Full dataset	**Total 2023**	1311	Reduced dataset	**Total 2023 - reduced**	396	
	Total 2024	866		**Total 2024**	267	
	Total Viewpoint A	756		**Total Viewpoint A**	58	
	Total Viewpoint B	563		**Total Viewpoint B**	164	
	Total Viewpoint C	878		**Total Viewpoint C**	441	

Appendix Table 2: Recording hours per month, season and year.

Month	**Recording hours**
January	453
February	315
March	481
April	725
May	657
June	725
July	896
August	1,042
September	1,394
October	781
November	317
December	466
Total recording hours	8,252
Total for Autumn	2,492
Total for Winter	1,234
Total for Spring	1,863
Total for Summer	2,663
Total for 2023	2,764

Total for 2024	5,488